PERGAMON

International Journal of Solids and Structures 38 (2001) 7769–7800

INTERNATIONAL JOURNAL OF SOLIDS and STRUCTURES

www.elsevier.com/locate/ijsolstr

Dual boundary element formulation for fracture mechanics analysis of shear deformable shells

T. Dirgantara [1], M.H. Aliabadi *

Department of Engineering, Queen Mary and Westfield College, University of London, Mile End, London E1 4NS, UK

Received 16 October 2000; in revised form 17 April 2001

Abstract

This paper presents a new boundary element formulation for fracture mechanics analysis of shear deformable shells. Hyper-singular boundary integral equations for shear deformable shells are derived. Dual boundary element formulations are constructed by using traction integral equations on one side of the crack surface and displacement integral equations on the other side of the crack surface and all other boundaries. Five stress intensity factors, two for membrane behaviour and three for shear and bending are computed. Several crack configurations are analysed to demonstrate the efficiency and accuracy of the proposed formulation.

Keywords: Fracture mechanics; Boundary element method; Shear deformable shells; Stress intensity factors

1. Introduction

Fracture mechanics analysis of shear deformable plates and shells has many important engineering applications, e.g. aircraft structure, pressure vessel and piping, and ship construction. The behaviour of cracked structure can be determined if the stress intensity factors of the problem are known, therefore during the last three decades much work has been done to evaluate stress intensity factor solutions for different loadings and geometries. Stress intensity factor solutions for several geometries of cylindrical and spherical shells have been presented in parametric form (Murakami et al., 1987) based on the classical theory (see e.g. Folias, 1965a,b; Erdogan and Kibler, 1968) as well as based on the shear deformable shell theory (see e.g. Sih and Hagendorf, 1977; Krenk, 1978; Delale and Erdogan, 1979a,b). However, due to the complexity of engineering structures, it is frequently necessary to perform numerical structural analysis.

* Corresponding author. Tel.: +44-20-7882-5301; fax: +44-20-8983-1007.
E-mail address: m.h.aliabadi@qmw.ac.uk (M.H. Aliabadi).
[1] On leave from Department of Aeronautical Engineering, Institut Teknologi Bandung, Jl. Ganesha 10, Bandung 40132, Indonesia.

0020-7683/01/$ - see front matter
PII: S0020-7683(01)00097-X

For the last two decades, finite element methods (FEM) have been developed to solve cracked shell problems (see e.g. Barsoum et al., 1979; Budiman and Lagace, 1997; Ehlers, 1986). More recently, boundary element method (BEM) has been emerged as an alternative numerical method for fracture mechanics analysis (see e.g. Portela and Aliabadi, 1992; Aliabadi, 1997a). The dual boundary element method (DBEM), which is based on displacement and traction integral equations, has been successfully developed to solve many applications of fracture mechanics problems e.g. 2D and 3D elasticity, thermoelastic, elastoplastic, stiffened panel, composite materials and dynamic fracture mechanics, as has been reviewed by Aliabadi (1997b). However, the application of the DBEM for analysis of crack in shells has not been reported previously.

The displacement boundary integral equations for the Reissner's plate model have been reported by Van der Weeën (1982) and Karam and Telles (1988). The traction integral equations for Reissner's plates have been reported by Rashed et al. (1998) in which they presented the complete derivation of the hyper-singular equations and demonstrated procedures for treating the hyper-singular integrals for general boundaries. Ahmadi-Brooghani and Wearing (1996) used those integral equations to form a DBEM formulation for crack analysis of plate bending involving shear deformation. Recently, Dirgantara and Aliabadi (2000) developed DBEM for crack growth analysis of plates loaded in combine bending and tension based on the Reissner's plate and 2-D plane stress elasticity theory.

The displacement boundary integral equation for shallow shells involving shear deformation was first reported by Lu and Huang (1992). Unfortunately, as described in Lu and Huang (1991), this technique involves complicated fundamental solutions. Using different approach called domain-BEM (see Beskos, 1991), Dirgantara and Aliabadi (1999) developed boundary integral equations for shear deformable shallow shells by coupling integral equations for shear deformable plate and 2-D plane stress elasticity. The fundamental solutions involved in this approach are the Reissner's plate fundamental solutions and the Kelvin fundamental solutions for plane stress which are much simpler then the previous technique developed by Lu and Huang (1991). However, this method contains domain integrals as well as boundary integrals. Utilizing direct integral method and dual reciprocity method (DRM), Wen et al. (2000), further developed this approach by transforming the domain integrals to boundary integrals.

In this paper, hyper-singular integral equations for shear deformable shells are derived. The hyper-singular integral equations together with displacement integral equations are employed to form DBEM formulation for fracture mechanics analysis of shear deformable shells. Several numerical examples are solved to demonstrate the accuracy and the use of the new dual integral equations.

2. Governing equations

Consider the shallow shell shown in Fig. 1. It has a quadratic middle surface given by

$$x_3 = -\tfrac{1}{2}(k_{11}x_1^2 + k_{22}x_2^2) \tag{2.1}$$

where $k_{11} = 1/R_1$ and $k_{22} = 1/R_2$ are principal curvatures of the shells, and R_1 and R_2 are radius of curvature of the shells in the x_1 and x_2 directions respectively.

The equilibrium equations of the shell are given by Sih and Hagendorf (1977) as follows:

$$M_{\alpha\beta,\beta} - Q_\alpha + m_\alpha = 0 \tag{2.2}$$

$$Q_{\alpha,\alpha} - k_{\alpha\beta}N_{\alpha\beta} + q_3 = 0 \tag{2.3}$$

$$N_{\alpha\beta,\beta} + q_\alpha = 0 \tag{2.4}$$

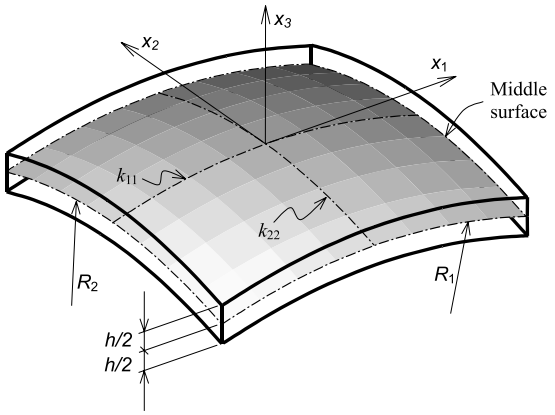

Fig. 1. Shallow shell having quadratic middle surface.

where $k_{12} = k_{21} = 0$. Throughout this paper indicial notation will be used. Roman indices vary from 1 to 3 and Greek indices vary from 1 to 2.

Stress-displacement relationships are given as

$$M_{\alpha\beta} = D\frac{1-v}{2}\left(w_{\alpha,\beta} + w_{\beta,\alpha} + \frac{2v}{1-v}w_{\gamma,\gamma}\delta_{\alpha\beta}\right) \tag{2.5}$$

$$Q_{\alpha} = D\frac{1-v}{2}\lambda^2(w_{\alpha} + w_{3,\alpha}) \tag{2.6}$$

$$N_{\alpha\beta} = B\frac{1-v}{2}\left(u_{\alpha,\beta} + u_{\beta,\alpha} + \frac{2v}{1-v}u_{\gamma,\gamma}\delta_{\alpha\beta}\right) + B\left[(1-v)k_{\alpha\beta} + v\delta_{\alpha\beta}k_{\phi\phi}\right]w_3 = N^{(\mathrm{i})}_{\alpha\beta} + N^{(\mathrm{ii})}_{\alpha\beta} \tag{2.7}$$

where u_α and w_3 are translation of displacements in x_1, x_2, x_3 direction respectively and w_α are rotations in x_1, x_2 direction respectively. $D(= Eh^3/[12(1-v^2)])$ is bending stiffness of the shell; $C(= \left[D(1-v)\lambda^2\right]/2)$ is shear stiffness; $B(= Eh/(1-v^2))$ is tension stiffness; $\lambda = \sqrt{10}/h$ is called the shear factor and h is the thickness of the shell. $M_{\alpha\beta}$ are bending moment stress resultants; Q_α are shear force stress resultants and $N_{\alpha\beta}$ are the normal force stress resultants. To make the integral representation more convenient, the term $N_{\alpha\beta}$ is separated to $N^{(\mathrm{i})}_{\alpha\beta}$ which are due to in-plane displacements and $N^{(\mathrm{ii})}_{\alpha\beta}$ which are due to curvature and out-of-plane displacements.

By substituting Eqs. (2.5)–(2.7) into Eqs. (2.2)–(2.4), the equilibrium equations in term of displacements are obtained as follows:

$$L^b_{ik}w_k + f^b_i = 0 \tag{2.8}$$

and

$$L^m_{\alpha\beta}u_\beta + f^m_\alpha = 0 \tag{2.9}$$

where L^b_{ik} is the Navier differential operator for shear deformable plate bending problems

$$L^b_{\alpha\beta} = \frac{D(1-v)}{2}\left[\left(\nabla^2 - \lambda^2\right)\delta_{\alpha\beta} + \frac{(1+v)}{(1-v)}\frac{\partial}{\partial x_\alpha}\frac{\partial}{\partial x_\beta}\right] \tag{2.10}$$

$$L^b_{\alpha 3} = -\frac{(1-v)D}{2}\lambda^2\frac{\partial}{\partial x_\alpha} \tag{2.11}$$

$$L^b_{3\alpha} = -L^b_{\alpha 3} \tag{2.12}$$

$$L^b_{33} = \frac{(1-\nu)D}{2}\lambda^2\nabla^2 \tag{2.13}$$

with $f^b_\alpha = 0$ and $f^b_3 = q^*_3$, while $L^m_{\alpha\beta}$ is the Navier differential operator for 2-D plane stress problems

$$L^m_{\alpha\beta} = B\nabla^2\delta_{\alpha\beta} + \frac{B(1+\nu)}{2}\frac{\partial}{\partial x_\alpha}\frac{\partial}{\partial x_\beta}\left(1-2\delta_{\alpha\beta}\right) \tag{2.14}$$

with $f^m_\alpha = q^*_\alpha$, where q^*_1, q^*_2, q^*_3 are equivalent body forces

$$q^*_1 = q_1 + B(k_{11}+\nu k_{22})\frac{\partial w_3}{\partial x_1} \tag{2.15}$$

$$q^*_2 = q_2 + B(\nu k_{11}+k_{22})\frac{\partial w_3}{\partial x_2} \tag{2.16}$$

$$q^*_3 = q_3 - B(k_{11}+\nu k_{22})\frac{\partial u_1}{\partial x_1} - B(\nu k_{11}+k_{22})\frac{\partial u_2}{\partial x_2} - B(k^2_{11}+k^2_{22}+2\nu k_{11}k_{22})w_3 \tag{2.17}$$

Eqs. (2.8) and (2.9) have the form of shear deformable plate bending and two-dimensional plane stress deformations respectively, for which boundary integral formulation procedures and fundamental solutions have already been developed (see Van der Weeën, 1982; Aliabadi and Rooke, 1991). Therefore boundary integral representation for those equations can be achieved by employing procedures for shear deformable plate bending and two-dimensional plane stress elasticity. The coupling terms consist of the force terms q^*_1, q^*_2, q^*_3 which should vanish for $k_{11} = k_{22} = 0$.

3. Displacement integral equations

The displacement integral equations for shear deformable shallow shell bending problems have been derived by using the weighted residual method to obtain five integral equations in term of displacements – two rotations, one out-of-plane displacement and two in-plane displacements in Dirgantara and Aliabadi (1999). With slightly different arrangements as written in Dirgantara and Aliabadi (1999), the displacement integral equations can be presented as follows:

$$\begin{aligned} w_i(\mathbf{X}') &+ \int_\Gamma P^*_{ij}(\mathbf{X}',\mathbf{x})w_j(\mathbf{x})\,\mathrm{d}\Gamma(\mathbf{x}) \\ &= \int_\Gamma W^*_{ij}(\mathbf{X}',\mathbf{x})p_j(\mathbf{x})\,\mathrm{d}\Gamma(\mathbf{x}) - \int_\Omega k_{\alpha\beta}B\frac{1-\nu}{2}\left(u_{\alpha,\beta}(\mathbf{X}) + u_{\beta,\alpha}(\mathbf{X}) + \frac{2\nu}{1-\nu}u_{\phi,\phi}(\mathbf{X})\delta_{\alpha\beta}\right)W^*_{i3}(\mathbf{X}',\mathbf{X})\,\mathrm{d}\Omega(\mathbf{X}) \\ &\quad - \int_\Omega k_{\alpha\beta}B\left((1-\nu)k_{\alpha\beta} + \nu\delta_{\alpha\beta}k_{\gamma\gamma}\right)w_3(\mathbf{X})W^*_{i3}(\mathbf{X}',\mathbf{X})\,\mathrm{d}\Omega(\mathbf{X}) \\ &\quad + \int_\Omega W^*_{i3}(\mathbf{X}',\mathbf{X})q_3(\mathbf{X})\,\mathrm{d}\Omega(\mathbf{X}) \end{aligned} \tag{3.1}$$

and

$$u_\theta(\mathbf{X}') + \int_\Gamma T^{(\mathrm{i})*}_{\theta\alpha}(\mathbf{X}',\mathbf{x})u_\alpha(\mathbf{x})\,\mathrm{d}\Gamma(\mathbf{x}) + \int_\Gamma U^*_{\theta\alpha}(\mathbf{x}',\mathbf{x})B\big[k_{\alpha\beta}(1-v)+v\delta_{\alpha\beta}k_{\phi\phi}\big]w_3(\mathbf{x})n_\beta(\mathbf{x})\,\mathrm{d}\Gamma(\mathbf{x})$$
$$- \int_\Omega U^*_{\theta\alpha}(\mathbf{X}',\mathbf{X})B\big[k_{\alpha\beta}(1-v)+v\delta_{\alpha\beta}k_{\phi\phi}\big]w_{3,\beta}(\mathbf{X})\,\mathrm{d}\Omega(\mathbf{X})$$
$$= \int_\Gamma U^*_{\theta\alpha}(\mathbf{X}',\mathbf{x})t_\alpha(\mathbf{x})\,\mathrm{d}\Gamma(\mathbf{x}) + \int_\Omega U^*_{\theta\alpha}(\mathbf{X}',\mathbf{X})q_\alpha\,\mathrm{d}\Omega(\mathbf{X}) \tag{3.2}$$

where $p_\alpha = M_{\alpha\beta}n_\beta$, $p_3 = Q_\alpha n_\alpha$, $t_\alpha = N_{\alpha\beta}n_\beta$, $t_\alpha = t^{(\mathrm{i})}_\alpha + t^{(\mathrm{ii})}_\alpha$, $\mathbf{x}\in\Gamma$ and $\mathbf{X}\in\Omega$ are field points on the boundary and inside the domain respectively, $W^*_{ij}(\mathbf{X}',\mathbf{x})$ and $U^*_{\theta\alpha}(\mathbf{X}',\mathbf{x})$ are the fundamental solutions for displacements, while $P^*_{ij}(\mathbf{X}',\mathbf{x})$ and $T^{(\mathrm{i})*}_{\theta\alpha}(\mathbf{X}',\mathbf{x})$ are the fundamental solutions for tractions. The expressions for these kernels are given in Dirgantara and Aliabadi (1999).

By taking the point $\mathbf{X}'$ to the boundary, that is $\mathbf{X}'\to\mathbf{x}'\in\Gamma$, and assuming that the displacements u_j satisfy Hölder continuity, Eq. (3.1) can be written as follows:

$$c_{ij}(\mathbf{x}')w_j(\mathbf{x}') + \cancel{\int}_\Gamma P^*_{ij}(\mathbf{x}',\mathbf{x})w_j(\mathbf{x})\,\mathrm{d}\Gamma(\mathbf{x})$$
$$= \int_\Gamma W^*_{ij}(\mathbf{x}',\mathbf{x})p_j(\mathbf{x})\,\mathrm{d}\Gamma(\mathbf{x}) - \int_\Omega W^*_{i3}(\mathbf{x}',\mathbf{X})\,k_{\alpha\beta}B\frac{1-v}{2}\left[u_{\alpha,\beta}(\mathbf{X}) + u_{\beta,\alpha}(\mathbf{X}) + \frac{2v}{1-v}u_{\phi,\phi}(\mathbf{X})\delta_{\alpha\beta}\right]\mathrm{d}\Omega(\mathbf{X})$$
$$- \int_\Omega W^*_{i3}(\mathbf{x}',\mathbf{X})k_{\alpha\beta}B\big((1-v)k_{\alpha\beta}+v\delta_{\alpha\beta}k_{\phi\phi}\big)w_3(\mathbf{X})\,\mathrm{d}\Omega(\mathbf{X})$$
$$+ \int_\Omega W^*_{i3}(\mathbf{x}',\mathbf{X})q_3(\mathbf{X})\,\mathrm{d}\Omega(\mathbf{X}) \tag{3.3}$$

and Eq. (3.2) can be written as

$$c_{\theta\alpha}(\mathbf{x}')u_\alpha(\mathbf{x}') + \cancel{\int}_\Gamma T^{*(\mathrm{i})}_{\theta\alpha}(\mathbf{x}',\mathbf{x})u_\alpha(\mathbf{x})\,\mathrm{d}\Gamma(\mathbf{x}) + \int_\Gamma U^*_{\theta\alpha}(\mathbf{x}',\mathbf{x})B\big[k_{\alpha\beta}(1-v)+v\delta_{\alpha\beta}k_{\phi\phi}\big]w_3(\mathbf{x})n_\beta(\mathbf{x})\,\mathrm{d}\Gamma(\mathbf{x})$$
$$- \int_\Omega U^*_{\theta\alpha}(\mathbf{x}',\mathbf{X})B\big[k_{\alpha\beta}(1-v)+v\delta_{\alpha\beta}k_{\phi\phi}\big]w_{3,\beta}(\mathbf{X})\,\mathrm{d}\Omega(\mathbf{X})$$
$$= \int_\Gamma U^*_{\theta\alpha}(\mathbf{x}',\mathbf{x})t_\alpha(\mathbf{x})\,\mathrm{d}\Gamma(\mathbf{x}) + \int_\Omega U^*_{\theta\alpha}(\mathbf{x}',\mathbf{X})q_\alpha(\mathbf{X})\,\mathrm{d}\Omega(\mathbf{X}) \tag{3.4}$$

where $\cancel{\int}$ denotes a Cauchy principal value integral, $\mathbf{x}'$, $\mathbf{x}\in\Gamma$ are source and field points respectively, and $c_{ij}(\mathbf{x}')$ are the jump terms. The value of $c_{ij}(\mathbf{x}')$ are

$$c_{ij}(\mathbf{x}') = \begin{cases} (1/2)\delta_{ij} & \text{for } \mathbf{x}'\in\Gamma \\ 1 & \text{for } \mathbf{X}'\in\Omega \end{cases} \tag{3.5}$$

4. Hyper-singular integral equations

The stress resultants at domain point $\mathbf{X}'$ can be evaluated from Eqs. (3.1) and (3.2) by using relationships in Eqs. (2.5)–(2.7) to give:

$$M_{\alpha\beta}(\mathbf{X}') = \int_\Gamma W^*_{\alpha\beta k}(\mathbf{X}',\mathbf{x})p_k(\mathbf{x})\,\mathrm{d}\Gamma(\mathbf{x}) - \int_\Gamma P^*_{\alpha\beta k}(\mathbf{X}',\mathbf{x})w_k(\mathbf{x})\,\mathrm{d}\Gamma(\mathbf{x}) + \int_\Omega W^*_{\alpha\beta 3}(\mathbf{X}',\mathbf{X})q^*_3\,\mathrm{d}\Omega(\mathbf{X}) \tag{4.1}$$

$$Q_\beta(\mathbf{X}') = \int_\Gamma W^*_{3\beta k}(\mathbf{X}',\mathbf{x})p_k(\mathbf{x})\,\mathrm{d}\Gamma(\mathbf{x}) - \int_\Gamma P^*_{3\beta k}(\mathbf{X}',\mathbf{x})w_k(\mathbf{x})\,\mathrm{d}\Gamma(\mathbf{x}) + \int_\Omega W^*_{3\beta 3}(\mathbf{X}',\mathbf{X})q^*_3\,\mathrm{d}\Omega(\mathbf{X}) \tag{4.2}$$

and

$$N_{\alpha\beta}(\mathbf{X}') = \int_\Gamma U^*_{\alpha\beta\gamma}(\mathbf{X}',\mathbf{x})t_\gamma(\mathbf{x})\,\mathrm{d}\Gamma(\mathbf{x}) - \int_\Gamma T^*_{\alpha\beta\gamma}(\mathbf{X}',\mathbf{x})u_\gamma(\mathbf{x})\,\mathrm{d}\Gamma(\mathbf{x}) - \int_\Gamma U^*_{\alpha\beta\gamma}(\mathbf{X}',\mathbf{x})B\big[k_{\alpha\gamma}(1-\nu)+\nu\delta_{\alpha\gamma}k_{\phi\phi}\big]w_3(\mathbf{x})n_\gamma(\mathbf{x})\,\mathrm{d}\Gamma(\mathbf{x}) + \int_\Omega U^*_{\alpha\beta\gamma}(\mathbf{X}',\mathbf{X})q^*_\gamma\,\mathrm{d}\Omega(\mathbf{X}) + B\big[(1-\nu)k_{\alpha\beta}+\nu\delta_{\alpha\beta}k_{\phi\phi}\big]w_3 \tag{4.3}$$

where the kernels $W^*_{i\beta k}$, $U^*_{\alpha\beta\gamma}$, $P^*_{i\beta k}$ and $T^*_{\alpha\beta\gamma}$ are given in Dirgantara and Aliabadi (2000).

The stress resultant boundary integral equations are formed by considering the behaviour of Eqs. (4.1)–(4.3) when the point $\mathbf{X}'$ approaches boundary Γ at $\mathbf{x}'$. To satisfy the continuity requirements, the point $\mathbf{x}'$ is assumed to be on a smooth boundary. A semi-circular domain with boundary Γ^*_ε is constructed around the point $\mathbf{x}'$ as shown in Fig. 2.

Taking the limit as $\mathbf{X}' \to \mathbf{x}'$, Eqs. (4.1)–(4.3) can be rewritten as follows:

$$M_{\alpha\beta}(\mathbf{x}') + \lim_{\varepsilon\to0}\int_{\Gamma-\Gamma_\varepsilon+\Gamma^*_\varepsilon} P^*_{\alpha\beta\gamma}(\mathbf{x}',\mathbf{x})w_\gamma(\mathbf{x})\,\mathrm{d}\Gamma(\mathbf{x}) + \lim_{\varepsilon\to0}\int_{\Gamma-\Gamma_\varepsilon+\Gamma^*_\varepsilon} P^*_{\alpha\beta3}(\mathbf{x}',\mathbf{x})w_3(\mathbf{x})\,\mathrm{d}\Gamma(\mathbf{x}) = \lim_{\varepsilon\to0}\int_{\Gamma-\Gamma_\varepsilon+\Gamma^*_\varepsilon} W^*_{\alpha\beta\gamma}(\mathbf{x}',\mathbf{x})p_\gamma(\mathbf{x})\,\mathrm{d}\Gamma(\mathbf{x}) + \lim_{\varepsilon\to0}\int_{\Gamma-\Gamma_\varepsilon+\Gamma^*_\varepsilon} W^*_{\alpha\beta3}(\mathbf{x}',\mathbf{x})p_3(\mathbf{x})\,\mathrm{d}\Gamma(\mathbf{x}) + \lim_{\varepsilon\to0}\int_\Omega W^*_{\alpha\beta3}(\mathbf{X}',\mathbf{X})q^*_3\,\mathrm{d}\Omega(\mathbf{X}) \tag{4.4}$$

$$Q_\beta(\mathbf{x}') + \lim_{\varepsilon\to0}\int_{\Gamma-\Gamma_\varepsilon+\Gamma^*_\varepsilon} P^*_{3\beta\gamma}(\mathbf{x}',\mathbf{x})w_\gamma(\mathbf{x})\,\mathrm{d}\Gamma(\mathbf{x}) + \lim_{\varepsilon\to0}\int_{\Gamma-\Gamma_\varepsilon+\Gamma^*_\varepsilon} P^*_{3\beta3}(\mathbf{x}',\mathbf{x})w_3(\mathbf{x})\,\mathrm{d}\Gamma(\mathbf{x}) = \lim_{\varepsilon\to0}\int_{\Gamma-\Gamma_\varepsilon+\Gamma^*_\varepsilon} W^*_{3\beta\gamma}(\mathbf{x}',\mathbf{x})p_\gamma(\mathbf{x})\,\mathrm{d}\Gamma(\mathbf{x}) + \lim_{\varepsilon\to0}\int_{\Gamma-\Gamma_\varepsilon+\Gamma^*_\varepsilon} W^*_{3\beta3}(\mathbf{x}',\mathbf{x})p_3(\mathbf{x})\,\mathrm{d}\Gamma(\mathbf{x}) + \lim_{\varepsilon\to0}\int_\Omega W^*_{3\beta3}(\mathbf{X}',\mathbf{X})q^*_3\,\mathrm{d}\Omega(\mathbf{X}) \tag{4.5}$$

and

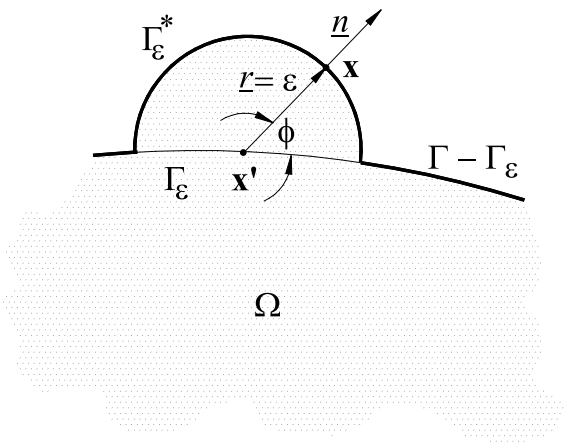

Fig. 2. Semi-circular region around the source point when it approaches the boundary.

$$
\begin{aligned}
&N_{\alpha\beta}(\mathbf{x}') + \lim_{\varepsilon\to 0}\int_{\Gamma-\Gamma_\varepsilon+\Gamma_\varepsilon^*} T^*_{\alpha\beta\gamma}(\mathbf{x}',\mathbf{x})u_\gamma(\mathbf{x})\,\mathrm{d}\Gamma(\mathbf{x}) \\
&\quad = \lim_{\varepsilon\to 0}\int_{\Gamma-\Gamma_\varepsilon+\Gamma_\varepsilon^*} U^*_{\alpha\beta\gamma}(\mathbf{x}',\mathbf{x})t_\gamma(\mathbf{x})\,\mathrm{d}\Gamma(\mathbf{x}) \\
&\qquad - \lim_{\varepsilon\to 0}\int_{\Gamma-\Gamma_\varepsilon+\Gamma_\varepsilon^*} U^*_{\alpha\beta\gamma}(\mathbf{X}',\mathbf{x})B\left[k_{\alpha\gamma}(1-\nu)+\nu\delta_{\alpha\gamma}k_{\phi\phi}\right]w_3(\mathbf{x})n_\gamma(\mathbf{x})\,\mathrm{d}\Gamma(\mathbf{x}) \\
&\qquad + \lim_{\varepsilon\to 0}\int_{\Omega} W^*_{\alpha\beta\gamma}(\mathbf{X}',\mathbf{X})q^*_\gamma\,\mathrm{d}\Omega(\mathbf{X}) + B\left[(1-\nu)k_{\alpha\beta}+\nu\delta_{\alpha\beta}k_{\phi\phi}\right]w_3
\end{aligned}
\tag{4.6}
$$

Eqs. (4.4) and (4.5) represent the bending moment and shear stress resultant boundary integral equations, respectively, while Eq. (4.6) represent the in-plane normal stress resultant boundary integral equations at the boundary point $\mathbf{x}'$.

In the limiting processes, w_i and u_α are required to be $C^{1,\alpha}$, $(0<\alpha<1)$, and p_i and t_α are required to be $C^{0,\alpha}$, $(0<\alpha<1)$, for the principal-value integrals to exist. Taking into consideration all the limits and the jump terms as in Dirgantara (2000), for a source point collocated on a smooth boundary the stress resultant integral equations are obtained as follows:

$$
\begin{aligned}
&\frac{1}{2}M_{\alpha\beta}(\mathbf{x}') + \cancel{\int}_\Gamma P^*_{\alpha\beta\gamma}(\mathbf{x}',\mathbf{x})u_\gamma(\mathbf{x})\,\mathrm{d}\Gamma(\mathbf{x}) + \int_\Gamma P^*_{\alpha\beta3}(\mathbf{x}',\mathbf{x})u_3(\mathbf{x})\,\mathrm{d}\Gamma(\mathbf{x}) \\
&\quad = \int_\Gamma W^*_{\alpha\beta\gamma}(\mathbf{x}',\mathbf{x})p_\gamma(\mathbf{x})\,\mathrm{d}\Gamma(\mathbf{x}) + \int_\Gamma W^*_{\alpha\beta3}(\mathbf{x}',\mathbf{x})p_3(\mathbf{x})\,\mathrm{d}\Gamma(\mathbf{x}) + \int_\Omega W^*_{\alpha\beta3}(\mathbf{x}',\mathbf{X})q^*_3\,\mathrm{d}\Omega(\mathbf{X})
\end{aligned}
\tag{4.7}
$$

$$
\begin{aligned}
&\frac{1}{2}Q_\beta(\mathbf{x}') + \int_\Gamma P^*_{3\beta\gamma}(\mathbf{x}',\mathbf{x})w_\gamma(\mathbf{x})\,\mathrm{d}\Gamma(\mathbf{x}) + \cancel{\int}_\Gamma P^*_{3\beta3}(\mathbf{x}',\mathbf{x})w_3(\mathbf{x})\,\mathrm{d}\Gamma(\mathbf{x}) \\
&\quad = \int_\Gamma W^*_{3\beta\gamma}(\mathbf{x}',\mathbf{x})p_\gamma(\mathbf{x})\,\mathrm{d}\Gamma(\mathbf{x}) + \int_\Gamma W^*_{3\beta3}(\mathbf{x}',\mathbf{x})p_3(\mathbf{x})\,\mathrm{d}\Gamma(\mathbf{x}) + \int_\Omega W^*_{3\beta3}(\mathbf{x}',\mathbf{X})q^*_3\,\mathrm{d}\Omega(\mathbf{X})
\end{aligned}
\tag{4.8}
$$

and

$$
\begin{aligned}
&\frac{1}{2}N_{\alpha\beta}(\mathbf{x}') + \cancel{\int}_\Gamma T^*_{\alpha\beta\gamma}(\mathbf{x}',\mathbf{x})u_\gamma(\mathbf{x})\,\mathrm{d}\Gamma(\mathbf{x}) + \int_\Gamma U^*_{\alpha\beta\gamma}(\mathbf{X}',\mathbf{x})B\left[k_{\alpha\gamma}(1-\nu)+\nu\delta_{\alpha\gamma}k_{\phi\phi}\right]w_3(\mathbf{x})n_\gamma(\mathbf{x})\,\mathrm{d}\Gamma(\mathbf{x}) \\
&\quad = \int_\Gamma U^*_{\alpha\beta\gamma}(\mathbf{x}',\mathbf{x})t_\gamma(\mathbf{x})\,\mathrm{d}\Gamma(\mathbf{x}) + \int_\Omega U^*_{\alpha\beta\gamma}(\mathbf{x}',\mathbf{X})q^*_\gamma\,\mathrm{d}\Omega(\mathbf{X}) + \frac{1}{2}B\left[(1-\nu)k_{\alpha\beta}+\nu\delta_{\alpha\beta}k_{\phi\phi}\right]w_3
\end{aligned}
\tag{4.9}
$$

5. Traction integral equations

If Eqs. (4.7)–(4.9) are multiplied by n_β at the collocation point $\mathbf{x}'$, and substituting Eqs. (2.15)–(2.17), the following integral equations can be written:

$$\begin{aligned}
&\frac{1}{2}p_\alpha(\mathbf{x}') + n_\beta(\mathbf{x}')\oint_\Gamma P^*_{\alpha\beta\gamma}(\mathbf{x}',\mathbf{x})u_\gamma(\mathbf{x})\,d\Gamma(\mathbf{x}) + n_\beta(\mathbf{x}')\oint_\Gamma P^*_{\alpha\beta3}(\mathbf{x}',\mathbf{x})u_3(\mathbf{x})\,d\Gamma(\mathbf{x})\\
&\quad = n_\beta(\mathbf{x}')\oint_\Gamma W^*_{\alpha\beta\gamma}(\mathbf{x}',\mathbf{x})p_\gamma(\mathbf{x})\,d\Gamma(\mathbf{x}) + n_\beta(\mathbf{x}')\int_\Gamma W^*_{\alpha\beta3}(\mathbf{x}',\mathbf{x})p_3(\mathbf{x})\,d\Gamma(\mathbf{x})\\
&\qquad - n_\beta(\mathbf{x}')\int_\Omega k_{\theta\psi}B\frac{1-v}{2}\left(u_{\theta,\psi}(\mathbf{X}) + u_{\psi,\theta}(\mathbf{X}) + \frac{2v}{1-v}u_{\phi,\phi}(\mathbf{X})\delta_{\theta\psi}\right)W^*_{\alpha\beta3}(\mathbf{x}',\mathbf{X})\,d\Omega(\mathbf{X})\\
&\qquad - n_\beta(\mathbf{x}')\int_\Omega k_{\theta\psi}B\big((1-v)k_{\theta\psi} + v\delta_{\theta\psi}k_{\phi\phi}\big)w_3(\mathbf{X})W^*_{\alpha\beta3}(\mathbf{x}',\mathbf{X})\,d\Omega(\mathbf{X}) + n_\beta(\mathbf{x}')\int_\Omega W^*_{\alpha\beta3}(\mathbf{x}',\mathbf{X})q_3\,d\Omega(\mathbf{X})
\end{aligned} \tag{5.1}$$

$$\begin{aligned}
&\frac{1}{2}p_3(\mathbf{x}') + n_\beta(\mathbf{x}')\oint_\Gamma P^*_{3\beta\gamma}(\mathbf{x}',\mathbf{x})u_\gamma(\mathbf{x})\,d\Gamma(\mathbf{x}) + n_\beta(\mathbf{x}')\oint_\Gamma P^*_{3\beta3}(\mathbf{x}',\mathbf{x})u_3(\mathbf{x})\,d\Gamma(\mathbf{x})\\
&\quad = n_\beta(\mathbf{x}')\int_\Gamma W^*_{3\beta\gamma}(\mathbf{x}',\mathbf{x})p_\gamma(\mathbf{x})\,d\Gamma(\mathbf{x}) + n_\beta(\mathbf{x}')\oint_\Gamma W^*_{3\beta3}(\mathbf{x}',\mathbf{x})p_3(\mathbf{x})\,d\Gamma(\mathbf{x})\\
&\qquad - n_\beta(\mathbf{x}')\int_\Omega k_{\theta\psi}B\frac{1-v}{2}\left(u_{\theta,\psi}(\mathbf{X}) + u_{\psi,\theta}(\mathbf{X}) + \frac{2v}{1-v}u_{\phi,\phi}(\mathbf{X})\delta_{\theta\psi}\right)W^*_{3\beta3}(\mathbf{x}',\mathbf{X})\,d\Omega(\mathbf{X})\\
&\qquad - n_\beta(\mathbf{x}')\int_\Omega k_{\theta\psi}B\big((1-v)k_{\theta\psi} + v\delta_{\theta\psi}k_{\phi\phi}\big)w_3(\mathbf{X})W^*_{3\beta3}(\mathbf{x}',\mathbf{X})\,d\Omega(\mathbf{X}) + n_\beta(\mathbf{x}')\int_\Omega W^*_{3\beta3}(\mathbf{x}',\mathbf{X})q_3\,d\Omega(\mathbf{X})
\end{aligned} \tag{5.2}$$

and

$$\begin{aligned}
&\frac{1}{2}t_\alpha(\mathbf{x}') + n_\beta(\mathbf{x}')\oint_\Gamma T^*_{\alpha\beta\gamma}(\mathbf{x}',\mathbf{x})u_\gamma(\mathbf{x})\,d\Gamma(\mathbf{x}) + n_\beta(\mathbf{x}')\oint_\Gamma U^*_{\alpha\beta\gamma}(\mathbf{x}',\mathbf{x})B\big[k_{\theta\psi}(1-v) + v\delta_{\theta\psi}k_{\phi\phi}\big]w_3(\mathbf{x})n_\psi(\mathbf{x})\,d\Gamma(\mathbf{x})\\
&\qquad - n_\beta(\mathbf{x}')\int_\Omega U^*_{\alpha\beta\gamma}(\mathbf{x}',\mathbf{X})B\big[k_{\theta\psi}(1-v) + v\delta_{\theta\psi}k_{\phi\phi}\big]w_{3,\beta}(\mathbf{X})\,d\Omega(\mathbf{X})\\
&\quad = n_\beta(\mathbf{x}')\oint_\Gamma U^*_{\alpha\beta\gamma}(\mathbf{x}',\mathbf{x})t_\gamma(\mathbf{x})\,d\Gamma(\mathbf{x}) + n_\beta(\mathbf{x}')\int_\Omega U^*_{\alpha\beta\gamma}(\mathbf{x}',\mathbf{X})q_\gamma\,d\Omega(\mathbf{X})\\
&\qquad + \frac{1}{2}n_\beta(\mathbf{x}')B\big[(1-v)k_{\theta\psi} + v\delta_{\theta\psi}k_{\phi\phi}\big]w_3(\mathbf{x}')
\end{aligned} \tag{5.3}$$

Eqs. (5.1)–(5.3) represent five integral equations in terms of boundary tractions, and can be used together with the five displacement integral equations in Eqs. (3.3) and (3.4) to form the dual boundary integral formulation.

6. Treatment of domain integrals using the dual reciprocity method

6.1. Displacement boundary integral equations

The transformation of domain integrals to boundary integrals for displacement boundary integral equations of shear deformable shells using the DRM will follow to those developed by Wen et al. (2000).

If the plane stress elasticity body forces $q_1 = q_2 = 0$, in the displacement boundary integral equations (3.3) and (3.4) there are six domain integrals as follows:

$$I_1^D = \int_\Omega W_{i3}^* w_3 \,\mathrm{d}\Omega, \quad I_2^D = \int_\Omega W_{i3}^* \frac{\partial u_1}{\partial x_1} \,\mathrm{d}\Omega,$$
$$I_3^D = \int_\Omega W_{i3}^* \frac{\partial u_2}{\partial x_2} \,\mathrm{d}\Omega, \quad I_4^D = \int_\Omega W_{i3}^* q_3 \,\mathrm{d}\Omega, \tag{6.1}$$
$$I_5^D = \int_\Omega U_{\alpha 1}^* \frac{\partial w_3}{\partial x_1} \,\mathrm{d}\Omega, \quad I_6^D = \int_\Omega U_{\alpha 2}^* \frac{\partial w_3}{\partial x_2} \,\mathrm{d}\Omega$$

From the particular solution $\hat{w}_{mk}^3$ for plate bending problem, which satisfy the differential equation,

$$L_{\alpha k}^{b,\mathrm{adj}} \hat{w}_{mk}^3 = 0 \text{ and } L_{3k}^{b,\mathrm{adj}} \hat{w}_{mk}^3 = F_m(r) \tag{6.2}$$

where $L_{\alpha k}^{b,\mathrm{adj}}$ and $L_{3k}^{b,\mathrm{adj}}$ are adjoint operator of original differential operator L_{ik}^b for plate bending, the boundary integral equations for plate bending problem becomes

$$c_{ik}(\mathbf{x}')\hat{w}_{mk}^3(\mathbf{x}') = \int_\Gamma W_{ik}^*(\mathbf{x}', \mathbf{x})\hat{p}_{mk}^3(\mathbf{x}) \,\mathrm{d}\Gamma(\mathbf{x}) - \oint_\Gamma P_{ik}^*(\mathbf{x}', \mathbf{x})\hat{w}_{mk}^3(\mathbf{x}) \,\mathrm{d}\Gamma(\mathbf{x}) + \int_\Omega W_{i3}^*(\mathbf{x}', \mathbf{X})F_m(r) \,\mathrm{d}\Omega(\mathbf{X}) \tag{6.3}$$

which implies that

$$I_1^D = \sum_{m=1}^{M} \left[c_{ik}(\mathbf{x}')\hat{w}_{mk}^3(\mathbf{x}') - \int_\Gamma W_{ik}^*(\mathbf{x}', \mathbf{x})\hat{p}_{mk}^3(\mathbf{x}) \,\mathrm{d}\Gamma(\mathbf{x}) + \oint_\Gamma P_{ik}^*(\mathbf{x}', \mathbf{x})\hat{w}_{mk}^3(\mathbf{x}) \,\mathrm{d}\Gamma(\mathbf{x}) \right] \mathbf{F}^{-1} w_3 \tag{6.4}$$

The particular solutions $\hat{w}_{mk}^3$ and $\hat{p}_{mk}^3$ for radial basis function $F_m(r) = 1 + r$ were derived in Wen et al. (2000) and are given in Appendix A. Similar to the previous procedure, if

$$L_{\alpha k}^{b,\mathrm{adj}} \hat{w}_{mk}^3 = 0 \text{ and } L_{3k}^{b,\mathrm{adj}} \hat{w}_{mk}^3 = \frac{\partial F_m(r)}{\partial x_\alpha} = \frac{x_\alpha}{r} \tag{6.5}$$

the domain integral

$$I_2^D = \sum_{m=1}^{M} \left[c_{ik}(\mathbf{x}')\hat{w}_{mk}^1(\mathbf{x}') - \int_\Gamma W_{ik}^*(\mathbf{x}', \mathbf{x})\hat{p}_{mk}^1(\mathbf{x}) \,\mathrm{d}\Gamma(\mathbf{x}) + \oint_\Gamma P_{ik}^*(\mathbf{x}', \mathbf{x})\hat{w}_{mk}^1(\mathbf{x}) \,\mathrm{d}\Gamma(\mathbf{x}) \right] \mathbf{F}^{-1} u_1 \tag{6.6}$$

and

$$I_3^D = \sum_{m=1}^{M} \left[c_{ik}(\mathbf{x}')\hat{w}_{mk}^2(\mathbf{x}') - \int_\Gamma W_{ik}^*(\mathbf{x}', \mathbf{x})\hat{p}_{mk}^2(\mathbf{x}) \,\mathrm{d}\Gamma(\mathbf{x}) + \oint_\Gamma P_{ik}^*(\mathbf{x}', \mathbf{x})\hat{w}_{mk}^2(\mathbf{x}) \,\mathrm{d}\Gamma(\mathbf{x}) \right] \mathbf{F}^{-1} u_2 \tag{6.7}$$

The particular solutions $\hat{w}_{mk}^\alpha$ and $\hat{p}_{mk}^\alpha$ are given in Appendix A. Domain integral I_4^D can be obtained from Eq. (6.4) by replacing w_3 with q.

I_5^D can be evaluated from the particular solutions $\hat{u}_{m\alpha}^1$ and $\hat{t}_{m\alpha}^1$ for 2-D plane stress elasticity problems, that is

$$L_{1\alpha}^{m,\mathrm{adj}} \hat{u}_{m\alpha}^1 = \frac{\partial F_m(r)}{\partial x_1} = \frac{x_1}{r} \text{ and } L_{2\alpha}^{m,\mathrm{adj}} \hat{u}_{m\alpha}^1 = 0 \tag{6.8}$$

to give

$$I_5^D = \sum_{m=1}^{M} \left[c_{\alpha\beta}(\mathbf{x}')\hat{u}_{m\beta}^1(\mathbf{x}') - \int_\Gamma U_{\alpha\beta}^*(\mathbf{x}', \mathbf{x})\hat{t}_{m\beta}^1(\mathbf{x}) \,\mathrm{d}\Gamma(\mathbf{x}) + \oint_\Gamma T_{\alpha\beta}^*(\mathbf{x}', \mathbf{x})\hat{u}_{m\beta}^1(\mathbf{x}) \,\mathrm{d}\Gamma(\mathbf{x}) \right] \mathbf{F}^{-1} w_3 \tag{6.9}$$

The last domain integral I_6^D can be obtained from the particular solutions $\hat{u}_{m\alpha}^2$ and $\hat{t}_{m\alpha}^2$ for 2-D plane stress elasticity problems, that is

$$L_{1\alpha}^{m,\mathrm{adj}} \hat{u}_{m\alpha}^2 = 0 \text{ and } L_{2\alpha}^{m,\mathrm{adj}} \hat{u}_{m\alpha}^2 = \frac{\partial F_m(r)}{\partial x_2} = \frac{x_2}{r} \tag{6.10}$$

to give

$$I_6^D = \sum_{m=1}^{M} \left[c_{\alpha\beta}(\mathbf{x}')\hat{u}^2_{m\beta}(\mathbf{x}') - \int_\Gamma U^*_{\alpha\beta}(\mathbf{x}',\mathbf{x})\hat{t}^2_{m\beta}(\mathbf{x})\,\mathrm{d}\Gamma(\mathbf{x}) + \oint_\Gamma T^*_{\alpha\beta}(\mathbf{x}',\mathbf{x})\hat{u}^2_{m\beta}(\mathbf{x})\,\mathrm{d}\Gamma(\mathbf{x}) \right] \mathbf{F}^{-1} w_3 \tag{6.11}$$

6.2. Traction integral equations

The transformation of domain integrals to boundary integrals for traction boundary integral equations of shear deformable shells using the DRM can be evaluated from the DRM results of the displacement boundary integral equations. In the traction boundary integral equations (5.1)–(5.3) there are six domain integrals as follows:

$$\begin{aligned}
&n_\beta(\mathbf{x}')I_7^D = n_\beta(\mathbf{x}') \int_\Omega W^*_{i\beta 3} w_3 \,\mathrm{d}\Omega, \quad n_\beta(\mathbf{x}')I_8^D = n_\beta(\mathbf{x}') \int_\Omega W^*_{i\beta 3} \frac{\partial u_1}{\partial x_1}\,\mathrm{d}\Omega,\\
&n_\beta(\mathbf{x}')I_9^D = n_\beta(\mathbf{x}') \int_\Omega W^*_{i\beta 3} \frac{\partial u_2}{\partial x_2}\,\mathrm{d}\Omega, \quad n_\beta(\mathbf{x}')I_{10}^D = n_\beta(\mathbf{x}') \int_\Omega W^*_{i\beta 3} q_3 \,\mathrm{d}\Omega,\\
&n_\beta(\mathbf{x}')I_{11}^D = n_\beta(\mathbf{x}') \int_\Omega U^*_{\alpha\beta 1} \frac{\partial w_3}{\partial x_1}\,\mathrm{d}\Omega, \quad n_\beta(\mathbf{x}')I_{12}^D = n_\beta(\mathbf{x}') \int_\Omega U^*_{\alpha\beta 2} \frac{\partial w_3}{\partial x_2}\,\mathrm{d}\Omega
\end{aligned} \tag{6.12}$$

Using the same particular solutions $\hat{w}^3_{mk}$ and $\hat{p}^3_{mk}$ as in displacement integral equations, the stress resultant integral equations for plate bending problems can be written as

$$\begin{aligned}
&\frac{1}{2}\hat{M}^3_{m\alpha\beta}(\mathbf{x}') + \oint_\Gamma P^*_{\alpha\beta\gamma}(\mathbf{x}',\mathbf{x})\hat{w}^3_{m\gamma}(\mathbf{x})\,\mathrm{d}\Gamma(\mathbf{x}) + \int_\Gamma P^*_{\alpha\beta 3}(\mathbf{x}',\mathbf{x})\hat{w}^3_{m3}(\mathbf{x})\,\mathrm{d}\Gamma(\mathbf{x})\\
&\quad = \int_\Gamma W^*_{\alpha\beta\gamma}(\mathbf{x}',\mathbf{x})\hat{p}^3_{m\gamma}(\mathbf{x})\,\mathrm{d}\Gamma(\mathbf{x}) + \int_\Gamma W^*_{\alpha\beta 3}(\mathbf{x}',\mathbf{x})\hat{p}^3_{m3}(\mathbf{x})\,\mathrm{d}\Gamma(\mathbf{x}) + \int_\Omega W^*_{\alpha\beta 3}(\mathbf{x}',\mathbf{X})F_m(r)\,\mathrm{d}\Omega(\mathbf{X})
\end{aligned} \tag{6.13}$$

and

$$\begin{aligned}
&\frac{1}{2}\hat{Q}^3_{m\beta}(\mathbf{x}') + \int_\Gamma P^*_{3\beta\gamma}(\mathbf{x}',\mathbf{x})\hat{w}^3_{m\gamma}(\mathbf{x})\,\mathrm{d}\Gamma(\mathbf{x}) + \oint_\Gamma P^*_{3\beta 3}(\mathbf{x}',\mathbf{x})\hat{w}^3_{m3}(\mathbf{x})\,\mathrm{d}\Gamma(\mathbf{x})\\
&\quad = \int_\Gamma W^*_{3\beta\gamma}(\mathbf{x}',\mathbf{x})\hat{p}^3_{m\gamma}(\mathbf{x})\,\mathrm{d}\Gamma(\mathbf{x}) + \int_\Gamma W^*_{3\beta 3}(\mathbf{x}',\mathbf{x})\hat{p}^3_{m3}(\mathbf{x})\,\mathrm{d}\Gamma(\mathbf{x}) + \int_\Omega W^*_{3\beta 3}(\mathbf{x}',\mathbf{X})F_m(r)\,\mathrm{d}\Omega(\mathbf{X})
\end{aligned} \tag{6.14}$$

which implies that

$$\begin{aligned}
n_\beta(\mathbf{x}')I_7^D = n_\beta(\mathbf{x}')\Bigg\{ \sum_{m=1}^{M} \Bigg[&\frac{1}{2}\hat{M}^3_{m\alpha\beta}(\mathbf{x}') + \oint_\Gamma P^*_{\alpha\beta\gamma}(\mathbf{x}',\mathbf{x})\hat{w}^3_{m\gamma}(\mathbf{x})\,\mathrm{d}\Gamma(\mathbf{x}) + \int_\Gamma P^*_{\alpha\beta 3}(\mathbf{x}',\mathbf{x})\hat{w}^3_{m3}(\mathbf{x})\,\mathrm{d}\Gamma(\mathbf{x})\\
&- \int_\Gamma W^*_{\alpha\beta\gamma}(\mathbf{x}',\mathbf{x})\hat{p}^3_{m\gamma}(\mathbf{x})\,\mathrm{d}\Gamma(\mathbf{x}) - \int_\Gamma W^*_{\alpha\beta 3}(\mathbf{x}',\mathbf{x})\hat{p}^3_{m3}(\mathbf{x})\,\mathrm{d}\Gamma(\mathbf{x}) \Bigg] \mathbf{F}^{-1} w_3 \Bigg\}
\end{aligned} \tag{6.15}$$

and

$$\begin{aligned}
n_\beta(\mathbf{x}')I_7^D = n_\beta(\mathbf{x}')\Bigg\{ \sum_{m=1}^{M} \Bigg[&\frac{1}{2}\hat{Q}^3_{m\beta}(\mathbf{x}') + \int_\Gamma P^*_{3\beta\gamma}(\mathbf{x}',\mathbf{x})\hat{w}^3_{m\gamma}(\mathbf{x})\,\mathrm{d}\Gamma(\mathbf{x}) + \oint_\Gamma P^*_{3\beta 3}(\mathbf{x}',\mathbf{x})\hat{w}^3_{m3}(\mathbf{x})\,\mathrm{d}\Gamma(\mathbf{x})\\
&- \int_\Gamma W^*_{3\beta\gamma}(\mathbf{x}',\mathbf{x})\hat{p}^3_{m\gamma}(\mathbf{x})\,\mathrm{d}\Gamma(\mathbf{x}) - \int_\Gamma W^*_{3\beta 3}(\mathbf{x}',\mathbf{x})\hat{p}^3_{m3}(\mathbf{x})\,\mathrm{d}\Gamma(\mathbf{x}) \Bigg] \mathbf{F}^{-1} w_3 \Bigg\}
\end{aligned} \tag{6.16}$$

Similar to the previous procedure for the particular solutions $\hat{w}^{\alpha}_{mk}$ and $\hat{p}^{\alpha}_{mk}$, the domain integral I^D_8

$$n_\beta(\mathbf{x}')I^D_8 = n_\beta(\mathbf{x}')\left\{\sum_{m=1}^{M}\left[\frac{1}{2}\hat{M}^1_{m\alpha\beta}(\mathbf{x}') + \oint\!\!\!\!\!\!-_{\Gamma} P^*_{\alpha\beta\gamma}(\mathbf{x}',\mathbf{x})\hat{w}^1_{m\gamma}(\mathbf{x})\,\mathrm{d}\Gamma(\mathbf{x}) + \oint_{\Gamma} P^*_{\alpha\beta 3}(\mathbf{x}',\mathbf{x})\hat{w}^1_{m3}(\mathbf{x})\,\mathrm{d}\Gamma(\mathbf{x})\right.\right.$$
$$\left.\left. - \oint\!\!\!\!\!\!-_{\Gamma} W^*_{\alpha\beta\gamma}(\mathbf{x}',\mathbf{x})\hat{p}^1_{m\gamma}(\mathbf{x})\,\mathrm{d}\Gamma(\mathbf{x}) - \int_{\Gamma} W^*_{\alpha\beta 3}(\mathbf{x}',\mathbf{x})\hat{p}^1_{m3}(\mathbf{x})\,\mathrm{d}\Gamma(\mathbf{x})\right]\mathbf{F}^{-1}u_1\right\} \tag{6.17}$$

and

$$n_\beta(\mathbf{x}')I^D_8 = n_\beta(\mathbf{x}')\left\{\sum_{m=1}^{M}\left[\frac{1}{2}\hat{Q}^1_{m\beta}(\mathbf{x}') + \oint_{\Gamma} P^*_{3\beta\gamma}(\mathbf{x}',\mathbf{x})\hat{w}^1_{m\gamma}(\mathbf{x})\,\mathrm{d}\Gamma(\mathbf{x}) + \oint\!\!\!\!\!\!-_{\Gamma} P^*_{3\beta 3}(\mathbf{x}',\mathbf{x})\hat{w}^1_{m3}(\mathbf{x})\,\mathrm{d}\Gamma(\mathbf{x})\right.\right.$$
$$\left.\left. - \int_{\Gamma} W^*_{3\beta\gamma}(\mathbf{x}',\mathbf{x})\hat{p}^1_{m\gamma}(\mathbf{x})\,\mathrm{d}\Gamma(\mathbf{x}) - \oint\!\!\!\!\!\!-_{\Gamma} W^*_{3\beta 3}(\mathbf{x}',\mathbf{x})\hat{p}^1_{m3}(\mathbf{x})\,\mathrm{d}\Gamma(\mathbf{x})\right]\mathbf{F}^{-1}u_1\right\} \tag{6.18}$$

The domain integral I^D_9

$$n_\beta(\mathbf{x}')I^D_9 = n_\beta(\mathbf{x}')\left\{\sum_{m=1}^{M}\left[\frac{1}{2}\hat{M}^2_{m\alpha\beta}(\mathbf{x}') + \oint\!\!\!\!\!\!-_{\Gamma} P^*_{\alpha\beta\gamma}(\mathbf{x}',\mathbf{x})\hat{w}^2_{m\gamma}(\mathbf{x})\,\mathrm{d}\Gamma(\mathbf{x}) + \oint_{\Gamma} P^*_{\alpha\beta 3}(\mathbf{x}',\mathbf{x})\hat{w}^2_{m3}(\mathbf{x})\,\mathrm{d}\Gamma(\mathbf{x})\right.\right.$$
$$\left.\left. - n_\beta(\mathbf{x}')\oint\!\!\!\!\!\!-_{\Gamma} W^*_{\alpha\beta\gamma}(\mathbf{x}',\mathbf{x})\hat{p}^2_{m\gamma}(\mathbf{x})\,\mathrm{d}\Gamma(\mathbf{x}) - \int_{\Gamma} W^*_{\alpha\beta 3}(\mathbf{x}',\mathbf{x})\hat{p}^2_{m3}(\mathbf{x})\,\mathrm{d}\Gamma(\mathbf{x})\right]\mathbf{F}^{-1}u_2\right\} \tag{6.19}$$

and

$$n_\beta(\mathbf{x}')I^D_9 = n_\beta(\mathbf{x}')\left\{\sum_{m=1}^{M}\left[\frac{1}{2}\hat{Q}^2_{m\beta}(\mathbf{x}') + \oint_{\Gamma} P^*_{3\beta\gamma}(\mathbf{x}',\mathbf{x})\hat{w}^2_{m\gamma}(\mathbf{x})\,\mathrm{d}\Gamma(\mathbf{x}) + \oint\!\!\!\!\!\!-_{\Gamma} P^*_{3\beta 3}(\mathbf{x}',\mathbf{x})\hat{w}^2_{m3}(\mathbf{x})\,\mathrm{d}\Gamma(\mathbf{x})\right.\right.$$
$$\left.\left. - n_\beta(\mathbf{x}')\int_{\Gamma} W^*_{3\beta\gamma}(\mathbf{x}',\mathbf{x})\hat{p}^2_{m\gamma}(\mathbf{x})\,\mathrm{d}\Gamma(\mathbf{x}) - \oint\!\!\!\!\!\!-_{\Gamma} W^*_{3\beta 3}(\mathbf{x}',\mathbf{x})\hat{p}^2_{m3}(\mathbf{x})\,\mathrm{d}\Gamma(\mathbf{x})\right]\mathbf{F}^{-1}u_2\right\} \tag{6.20}$$

Domain integral I^D_{10} can be obtained from Eqs. (6.15) and (6.16) by replacing w_3 with q_3 to give

$$n_\beta(\mathbf{x}')I^D_{10} = n_\beta(\mathbf{x}')\left\{\sum_{m=1}^{M}\left[\frac{1}{2}\hat{M}^3_{m\alpha\beta}(\mathbf{x}') + \oint\!\!\!\!\!\!-_{\Gamma} P^*_{\alpha\beta\gamma}(\mathbf{x}',\mathbf{x})\hat{w}^3_{m\gamma}(\mathbf{x})\,\mathrm{d}\Gamma(\mathbf{x}) + \oint_{\Gamma} P^*_{\alpha\beta 3}(\mathbf{x}',\mathbf{x})\hat{w}^3_{m3}(\mathbf{x})\,\mathrm{d}\Gamma(\mathbf{x})\right.\right.$$
$$\left.\left. - \oint\!\!\!\!\!\!-_{\Gamma} W^*_{\alpha\beta\gamma}(\mathbf{x}',\mathbf{x})\hat{p}^3_{m\gamma}(\mathbf{x})\,\mathrm{d}\Gamma(\mathbf{x}) - \int_{\Gamma} W^*_{\alpha\beta 3}(\mathbf{x}',\mathbf{x})\hat{p}^3_{m3}(\mathbf{x})\,\mathrm{d}\Gamma(\mathbf{x})\right]\mathbf{F}^{-1}q_3\right\} \tag{6.21}$$

and

$$n_\beta(\mathbf{x}')I^D_{10} = n_\beta(\mathbf{x}')\left\{\sum_{m=1}^{M}\left[\frac{1}{2}\hat{Q}^3_{m\beta}(\mathbf{x}') + \oint_{\Gamma} P^*_{3\beta\gamma}(\mathbf{x}',\mathbf{x})\hat{w}^3_{m\gamma}(\mathbf{x})\,\mathrm{d}\Gamma(\mathbf{x}) + \oint\!\!\!\!\!\!-_{\Gamma} P^*_{3\beta 3}(\mathbf{x}',\mathbf{x})\hat{w}^3_{m3}(\mathbf{x})\,\mathrm{d}\Gamma(\mathbf{x})\right.\right.$$
$$\left.\left. - \int_{\Gamma} W^*_{3\beta\gamma}(\mathbf{x}',\mathbf{x})\hat{p}^3_{m\gamma}(\mathbf{x})\,\mathrm{d}\Gamma(\mathbf{x}) - \oint\!\!\!\!\!\!-_{\Gamma} W^*_{3\beta 3}(\mathbf{x}',\mathbf{x})\hat{p}^3_{m3}(\mathbf{x})\,\mathrm{d}\Gamma(\mathbf{x})\right]\mathbf{F}^{-1}q_3\right\} \tag{6.22}$$

I^D_{11} can be evaluated from the particular solutions $\hat{u}^1_{m\alpha}$ and $\hat{t}^1_{m\alpha}$ for two-dimensional plane stress elasticity problem, to give

$$n_\beta(\mathbf{x}')I_{11}^D = n_\beta(\mathbf{x}')\left\{\sum_{m=1}^{M}\left[\frac{1}{2}\hat{N}_{m\alpha\beta}^1(\mathbf{x}') - \int_\Gamma U_{\alpha\beta\gamma}^*(\mathbf{x}',\mathbf{x})\hat{t}_{m\gamma}^1(\mathbf{x})\,\mathrm{d}\Gamma(\mathbf{x}) + \oint_\Gamma T_{\alpha\beta\gamma}^{(\mathrm{i})*}(\mathbf{x}',\mathbf{x})\hat{u}_{m\gamma}^1(\mathbf{x})\,\mathrm{d}\Gamma(\mathbf{x})\right]\mathbf{F}^{-1}w_3\right\} \tag{6.23}$$

The last domain integral I_{12}^D can be obtained from the particular solution $\hat{u}_{m\alpha}^2$ and $\hat{t}_{m\alpha}^2$, to give

$$n_\beta(\mathbf{x}')I_{12}^D = n_\beta(\mathbf{x}')\left\{\sum_{m=1}^{M}\left[\frac{1}{2}\hat{N}_{m\alpha\beta}^2(\mathbf{x}') - \int_\Gamma U_{\alpha\beta\gamma}^*(\mathbf{x}',\mathbf{x})\hat{t}_{m\gamma}^2(\mathbf{x})\,\mathrm{d}\Gamma(\mathbf{x}) + \oint_\Gamma T_{\alpha\beta\gamma}^{(\mathrm{i})*}(\mathbf{x}',\mathbf{x})\hat{u}_{m\gamma}^2(\mathbf{x})\,\mathrm{d}\Gamma(\mathbf{x})\right]\mathbf{F}^{-1}w_3\right\} \tag{6.24}$$

7. Dual boundary element method

The dual equations, on which the DBEM is based, are the displacement and the traction boundary integral equations. Consider a cracked body shown in Fig. 3 with Γ^+, Γ^- referring to the upper and lower crack surfaces respectively and Γ^{e} denotes the rest of the boundary. The integral representation of the displacement components w_i and u_α are used for collocation points on the upper crack surface, that is $\mathbf{x}^+ \in \Gamma^+$, and the traction integral equations are used for collocation points on the lower crack surface. As the source point $\mathbf{x}^+$ is coincident with $\mathbf{x}^- \in \Gamma^-$, the extra free terms $(1/2)w_j(\mathbf{x}^-)$ and $(1/2)u_\alpha(\mathbf{x}^-)$ appear in Eqs. (3.3) and (3.4) and $-(1/2)p_j(\mathbf{x}^+)$ and $-(1/2)t_\alpha(\mathbf{x}^+)$ appear in Eqs. (5.1)–(5.3).

It is also important to note that in the DBEM, extra free terms will appear in I_1^D–I_{12}^D.

8. Numerical implementation

8.1. Modelling strategy

The general modelling strategy used in this work is similar with the one developed in Dirgantara and Aliabadi (2000). The strategy can be summarized as follows:

- crack boundaries are modelled with discontinuous quadratic elements, as shown in Fig. 4 to satisfy continuity conditions of displacements and its derivatives on all nodes for the existence of principal value integrals;
- the traction equations (5.1)–(5.3) are applied for collocation on one of the crack surfaces;

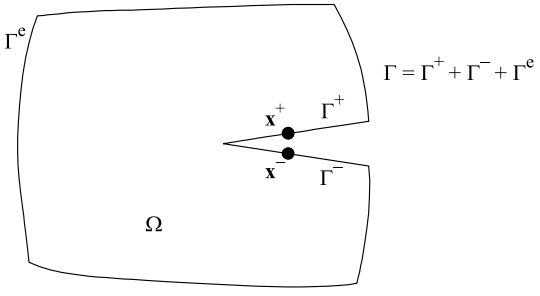

Fig. 3. A body contains a crack.

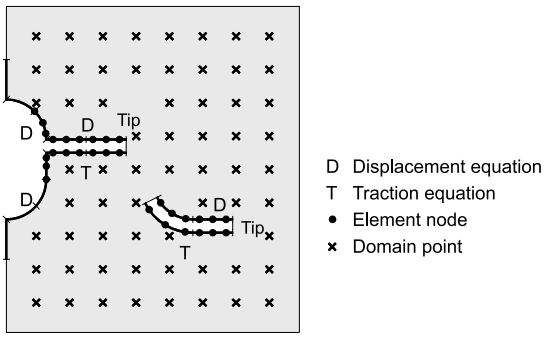

Fig. 4. Modelling strategy for dual boundary element of shear deformable shell.

- the displacement equations (3.3) and (3.4) are applied for collocation on the opposite crack surface and the other non-crack boundaries;
- continuous quadratic elements are applied along the remaining boundary of the body, except at the intersection between a crack and an edge, where discontinuous or semi-discontinuous are required on the edge in order to avoid a common node at intersection, and also at boundary corner, where semi-discontinuous are used in order to avoid a common node at the corner.
- several DRM collocation points are placed in the domain.

This simple strategy allows the DBEM to effectively model general crack problems.
After discretisation, Eqs. (3.3) and (3.4) together with Eqs. (5.1)–(5.3) can be written as

$$\begin{bmatrix} \mathbf{H}^{\mathrm{p}} + \mathbf{H}^{\mathrm{mod}} & \mathbf{H}^{\mathrm{u}} \\ \mathbf{H}^{\mathrm{w}} & \mathbf{H}^{\mathrm{e}} \end{bmatrix} \begin{Bmatrix} \mathbf{w} \\ \mathbf{u} \end{Bmatrix} = \begin{bmatrix} \mathbf{G}^{\mathrm{p}} & 0 \\ 0 & \mathbf{G}^{\mathrm{e}} \end{bmatrix} \begin{Bmatrix} \mathbf{p} \\ \mathbf{t} \end{Bmatrix} + \begin{Bmatrix} \mathbf{b} \\ 0 \end{Bmatrix} \tag{8.1}$$

where $\mathbf{w} = \{w_1, w_2, w_3\}^{\mathrm{T}}$, $\mathbf{u} = \{u_1, u_2\}^{\mathrm{T}}$ are the boundary displacement vectors, the vectors $\mathbf{p} = \{p_1, p_2, p_3\}^{\mathrm{T}}$, $\mathbf{t} = \{t_1, t_2\}^{\mathrm{T}}$ are the boundary traction vectors, $\mathbf{H}^{\mathrm{p}}$, $\mathbf{G}^{\mathrm{p}}$, $\mathbf{H}^{\mathrm{e}}$, and $\mathbf{G}^{\mathrm{e}}$ are the boundary element influence matrices for plate bending and plane stress elasticity respectively, $\mathbf{H}^{\mathrm{u}}$ and $\mathbf{H}^{\mathrm{w}}$ are coupling matrices of shallow shell, $\mathbf{H}^{\mathrm{mod}}$ is an additional matrix caused by the shell curvature, and $\mathbf{b}$ is the domain load vector. After imposing boundary condition, Eq. (4.4) can be written as

$$[A]_{5Nn\times 5Nn}\{x\}_{5Nn\times 1} = \{b\}_{5Nn\times 1} \tag{8.2}$$

where $[A]$ is the system matrix, $\{x\}$ is the unknown vector and $\{b\}$ is the vector of prescribed boundary values. Nn are number of boundary nodes plus domain points. Using LU decomposition, this system of algebraic equations can be solved for the boundary unknowns.

8.2. Special crack tip elements

To accurately model the displacement field $\sqrt{r}$ near the crack tip, a set of special shape function (similar to those by Mi and Aliabadi (1994) for three-dimensional elasticity problems) has been used. In this work, discontinuous quadratic elements with $\xi = -2/3,\ 0,\ +2/3$ are used. The variation of the displacements along the element is required to have the form of $u(\xi) = u^{\alpha}N^{\alpha}(\xi) = a_1^{\alpha} + a_2^{\alpha}\sqrt{r} + a_3^{\alpha}(r)$. If the crack tip is located at $\xi = -1$, then the shape function in the form $N^{\alpha}(\xi) = a_1^{\alpha} + a_2^{\alpha}\sqrt{1+\xi} + a_3^{\alpha}(1+\xi)$ is used. On the other hand, if the crack tip is located at $\xi = +1$, then the shape function in the form $N^{\alpha}(\xi) = b_1^{\alpha} + b_2^{\alpha}\sqrt{1-\xi} + b_3^{\alpha}(1-\xi)$ is used. If $N^{\alpha}(\xi)$ is set to be equal to δ_{α} (= 1 at the collocation node α and = 0 at the

other nodes), a set of linear system of equations can be established and the unknown constants can be obtained.

Finally, the shape functions for crack tip elements with the crack tip located at $\xi = -1$ are given by:

$$N_1(\xi) = \frac{3}{2}\frac{\left(3-\sqrt{15}\right)\xi + 2\sqrt{1+\xi} - 2}{\sqrt{15}+\sqrt{3}-6} \tag{8.3}$$

$$N_2(\xi) = \frac{3\left(\sqrt{15}-\sqrt{3}\right)\xi - 12\sqrt{1+\xi} + 2\left(\sqrt{15}+\sqrt{3}\right)}{2\left(\sqrt{15}+\sqrt{3}-6\right)} \tag{8.4}$$

$$N_3(\xi) = \frac{3}{2}\frac{\left(\sqrt{3}-3\right)\xi + 2\sqrt{1+\xi} - 2}{\sqrt{15}+\sqrt{3}-6} \tag{8.5}$$

and for crack tip element with the crack tip located at $\xi = +1$ are

$$N_1(\xi) = \frac{3}{2}\frac{\left(3-\sqrt{3}\right)\xi + 2\sqrt{1-\xi} - 2}{\sqrt{15}+\sqrt{3}-6} \tag{8.6}$$

$$N_2(\xi) = \frac{3\left(\sqrt{3}-\sqrt{15}\right)\xi - 12\sqrt{1-\xi} + 2\left(\sqrt{15}+\sqrt{3}\right)}{2\left(\sqrt{15}+\sqrt{3}-6\right)} \tag{8.7}$$

$$N_3(\xi) = \frac{3}{2}\frac{\left(\sqrt{15}-3\right)\xi + 2\sqrt{1-\xi} - 2}{\sqrt{15}+\sqrt{3}-6} \tag{8.8}$$

8.3. Singularities

There are three different orders of singularity that occur in the boundary integral equations, i.e. weak singular, strong singular and hyper-singular integrals. The treatment of these singular integrals have been reported as in Dirgantara and Aliabadi (2000) and are summarized below.

The weakly singular integrals are cancelled using a non-linear coordinate transformation as in Telles (1987). Strongly singular integrals at non-crack boundaries are evaluated indirectly using the generalised rigid body movements.

On the crack surface, the strong singular and hyper-singular integrals are evaluated using a singularity subtraction method based on the Taylor series expansion of the fundamental solution terms around the singular point, as in Aliabadi et al. (1985). Subsequently, the singular terms are integrated analytically.

8.4. Modelling consideration of the dual reciprocity technique

There are some difficulties in implementing the DRM technique for the DBEM analysis, due to the coincidence nodes along crack surfaces. These difficulties are summarized as follows:

(1) The DRM collocation points at crack boundaries. The existence of two coincident collocation points would make the DRM coefficient matrix becomes singular and requires a special treatment.

(2) Integrating over crack boundaries. In an incremental crack growth analysis, the inclusion of crack boundary implies that the boundary Γ is continuously changing from one incremental analysis to the next, and consequently the coefficient matrix has to be updated after each increment.

Similar to the argument reported in Salgado and Aliabadi (1998), the contribution of the integration over crack boundaries can be calculated by considering a collocation point $\mathbf{x}'$ and two coincidence nodes $\mathbf{x}^-$ and $\mathbf{x}^+$ on opposite crack surfaces. The integrals can be written in matrix form as

$$\Psi = \left[\mathbf{H}(\mathbf{x}',\mathbf{x}^+) \quad \mathbf{H}(\mathbf{x}',\mathbf{x}^-)\right]\begin{Bmatrix}\hat{\mathbf{w}}_k(\mathbf{x}',\mathbf{x}^+)\\ \hat{\mathbf{w}}_k(\mathbf{x}',\mathbf{x}^-)\end{Bmatrix} - \left[\mathbf{G}(\mathbf{x}',\mathbf{x}^+) \quad \mathbf{G}(\mathbf{x}',\mathbf{x}^-)\right]\begin{Bmatrix}\hat{p}_k(\mathbf{x}',\mathbf{x}^+)\\ \hat{p}_k(\mathbf{x}',\mathbf{x}^-)\end{Bmatrix} \tag{8.9}$$

It can be observed that particular solutions and fundamental solutions have properties as follows:

$$\begin{aligned}
&\hat{p}_k(\mathbf{x}',\mathbf{x}^+) = -\hat{p}_k(\mathbf{x}',\mathbf{x}^-); \quad \text{and} \quad \hat{t}_\beta(\mathbf{x}',\mathbf{x}^+) = -\hat{t}_\beta(\mathbf{x}',\mathbf{x}^-)\\
&\hat{w}_k(\mathbf{x}',\mathbf{x}^+) = \hat{w}_k(\mathbf{x}',\mathbf{x}^-); \quad \text{and} \quad \hat{u}_\beta(\mathbf{x}',\mathbf{x}^+) = \hat{u}_\beta(\mathbf{x}',\mathbf{x}^-)\\
&P^*_{ik}(\mathbf{x}',\mathbf{x}^+) = -P^*_{ik}(\mathbf{x}',\mathbf{x}^-); \quad \text{and} \quad T^*_{\alpha\beta}(\mathbf{x}',\mathbf{x}^+) = -T^*_{\alpha\beta}(\mathbf{x}',\mathbf{x}^-)\\
&P^*_{i\beta k}(\mathbf{x}',\mathbf{x}^+) = -P^*_{i\beta k}(\mathbf{x}',\mathbf{x}^-); \quad \text{and} \quad T^*_{\alpha\beta\gamma}(\mathbf{x}',\mathbf{x}^+) = -T^*_{\alpha\beta\gamma}(\mathbf{x}',\mathbf{x}^-)\\
&W^*_{ik}(\mathbf{x}',\mathbf{x}^+) = W^*_{ik}(\mathbf{x}',\mathbf{x}^-); \quad \text{and} \quad U^*_{\alpha\beta}(\mathbf{x}',\mathbf{x}^+) = U^*_{\alpha\beta}(\mathbf{x}',\mathbf{x}^-)\\
&W^*_{i\beta k}(\mathbf{x}',\mathbf{x}^+) = W^*_{i\beta k}(\mathbf{x}',\mathbf{x}^-); \quad \text{and} \quad U^*_{\alpha\beta\gamma}(\mathbf{x}',\mathbf{x}^+) = U^*_{\alpha\beta\gamma}(\mathbf{x}',\mathbf{x}^-)
\end{aligned} \tag{8.10}$$

Substituting properties in Eq. (8.10) into the matrix in Eq. (8.9), it can be seen that the contribution of the integration over crack boundaries to the coefficient matrix is equal to zero. Therefore, it is not necessary to include the crack boundaries in the integration process of I_1^D–I_{12}^D. In that case, the difficulties mentioned above are eliminated since the exclusion of crack boundary also means that there will be no DRM collocation points along the crack boundaries.

9. Evaluation of the stress intensity factors

Five stress intensity factors, two SIFs due to membrane loads and three due to bending moments and shear loads as shown in Fig. 5 have to be computed. In this work, the stress intensity factors are determined

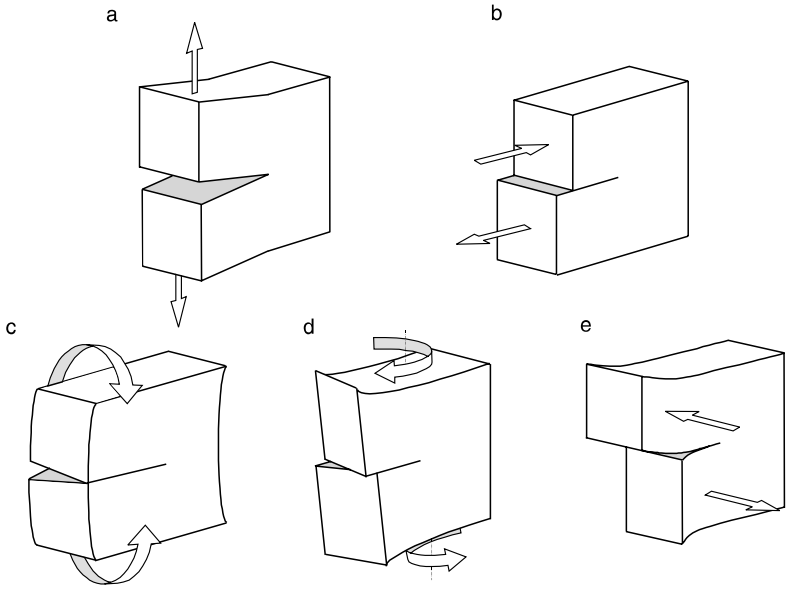

Fig. 5. Crack modes for shear deformable shell: (a) opening due to membrane stress resultant; (b) sliding due to membrane stress resultant; (c) opening due to bending stress resultant; (d) sliding due to bending stress resultant; (e) tearing due to shear stress resultant.

by the crack surface displacement extrapolation (CSDE) technique. The displacements field for shear deformable shell are as follows:

$$\begin{aligned}
\varphi_1 &= \frac{1+\nu}{E}\left(\frac{12}{h^3}\right)\sqrt{\frac{r}{2\pi}}\left[K_{1b}\cos\frac{\theta}{2}\left(\frac{3-\nu}{1+\nu}-\cos\theta\right)+K_{2b}\sin\frac{\theta}{2}\left(\frac{5+\nu}{1+\nu}-\cos\theta\right)\right]\\
\varphi_2 &= \frac{1+\nu}{E}\left(\frac{12}{h^3}\right)\sqrt{\frac{r}{2\pi}}\left[K_{1b}\sin\frac{\theta}{2}\left(\frac{3-\nu}{1+\nu}-\cos\theta\right)+K_{2b}\cos\frac{\theta}{2}\left(\frac{1-3\nu}{1+\nu}-\cos\theta\right)\right]\\
w_3 &= \frac{24(1+\nu)}{5Eh}\sqrt{\frac{r}{2\pi}}K_{3b}\sin\frac{\theta}{2}\\
u_1 &= \frac{2(1+\nu)}{Eh}\sqrt{\frac{r}{2\pi}}\left[K_{1m}\cos\frac{\theta}{2}\left(\frac{1-\nu}{1+\nu}+\sin^2\frac{\theta}{2}\right)+K_{2m}\sin\frac{\theta}{2}\left(\frac{2}{1+\nu}+\cos^2\frac{\theta}{2}\right)\right]\\
u_2 &= \frac{2(1+\nu)}{Eh}\sqrt{\frac{r}{2\pi}}\left[K_{1m}\sin\frac{\theta}{2}\left(\frac{2}{1+\nu}-\cos^2\frac{\theta}{2}\right)+K_{2m}\cos\frac{\theta}{2}\left(\frac{\nu-1}{1+\nu}+\sin^2\frac{\theta}{2}\right)\right]
\end{aligned} \tag{9.1}$$

where (r,θ) are the polar coordinates measured from the crack tip, K_{1m} and K_{2m} are mode I and mode II membrane stress resultant intensity factors respectively, K_{1b}, K_{2b}, and K_{3b} are two bending and shear stress resultant intensity factors respectively.

It is worth noting that the angular functions of the bending and membrane stress resultants for shear deformable plates and shells around the crack tip are identical. This feature permits the bending and membrane stress fields to be combined.

Reissner (1947) and Naghdi (1956) assumed that the stresses due to membrane forces are uniform, the stresses due to bending and twisting moments vary linearly and the transverse shear stresses vary parabolically over the thickness, and proposed expressions for the stress components as follows:

$$\left(1+\frac{x_3}{R_\gamma}\right)\sigma_{\alpha\beta}=\frac{1}{h}N_{\alpha\beta}+\frac{12x_3}{h^3}M_{\alpha\beta},\quad \begin{cases}\gamma=\beta \text{ if } \alpha\neq\beta\\ \gamma\neq\beta \text{ if } \alpha=\beta\end{cases} \tag{9.2}$$

and

$$\left(1+\frac{x_3}{R_\gamma}\right)\sigma_{\alpha 3}=\frac{3}{2h}\left[1-\left(\frac{2x_3}{h}\right)^2\right]Q_\alpha,\quad \gamma\neq\alpha \tag{9.3}$$

By considering Eqs. (9.2) and (9.3), relationships between the stress resultant intensity factors and the stress resultants, and also between the stress intensity factors and the stresses, the above stress resultant intensity factors can be related to stress intensity factors K_{I}, K_{II}, and K_{III} through the following relationships

$$\left[1+\frac{x_3}{2}\left(\frac{1}{R_1}+\frac{1}{R_2}\right)\right]K_{\mathrm{I}}=\frac{1}{h}K_{1m}+\frac{12x_3}{h^3}K_{1b} \tag{9.4}$$

$$\left[1+\frac{x_3}{2}\left(\frac{1}{R_1}+\frac{1}{R_2}\right)\right]K_{\mathrm{II}}=\frac{1}{h}K_{2m}+\frac{12x_3}{h^3}K_{2b} \tag{9.5}$$

and

$$\left[1+\frac{x_3}{2}\left(\frac{1}{R_1}+\frac{1}{R_2}\right)\right]K_{\mathrm{III}}=\frac{3}{2h}\left[1-\left(\frac{2x_3}{h}\right)^2\right]K_{3b} \tag{9.6}$$

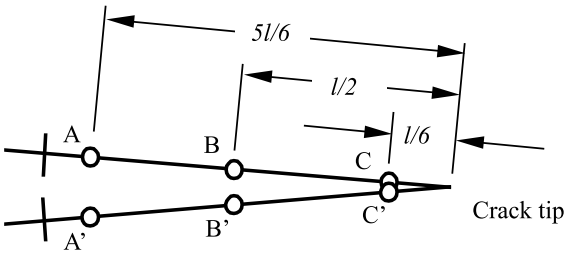

Fig. 6. Crack tip element.

The crack opening displacements are defined as:

$$\begin{Bmatrix} \Delta\varphi_1 \\ \Delta\varphi_2 \\ \Delta w_3 \\ \Delta u_1 \\ \Delta u_2 \end{Bmatrix} = \begin{Bmatrix} \varphi_1 \\ \varphi_2 \\ w_3 \\ u_1 \\ u_2 \end{Bmatrix}_{\theta=180^0} - \begin{Bmatrix} \varphi_1 \\ \varphi_2 \\ w_3 \\ u_1 \\ u_2 \end{Bmatrix}_{\theta=-180^0} \tag{9.7}$$

$$= \begin{bmatrix} \frac{48}{Eh^3}\sqrt{\frac{2r}{\pi}} & 0 & 0 & 0 & 0 \\ 0 & \frac{48}{Eh^3}\sqrt{\frac{2r}{\pi}} & 0 & 0 & 0 \\ 0 & 0 & \frac{24(1+\nu)}{5Eh}\sqrt{\frac{2r}{\pi}} & 0 & 0 \\ 0 & 0 & 0 & \frac{8}{Eh}\sqrt{\frac{r}{2\pi}} & 0 \\ 0 & 0 & 0 & 0 & \frac{8}{Eh}\sqrt{\frac{r}{2\pi}} \end{bmatrix} \begin{Bmatrix} K_{1b} \\ K_{2b} \\ K_{3b} \\ K_{1m} \\ K_{2m} \end{Bmatrix}$$

The stress intensity factors can be written in term of crack opening displacements, as

$$\begin{Bmatrix} K_{1b} \\ K_{2b} \\ K_{3b} \\ K_{1m} \\ K_{2m} \end{Bmatrix} = \frac{1}{\sqrt{r}} \begin{bmatrix} \frac{Eh^3}{48}\sqrt{\frac{\pi}{2}} & 0 & 0 & 0 & 0 \\ 0 & \frac{Eh^3}{48}\sqrt{\frac{\pi}{2}} & 0 & 0 & 0 \\ 0 & 0 & \frac{5Eh}{24(1+\nu)}\sqrt{\frac{\pi}{2}} & 0 & 0 \\ 0 & 0 & 0 & \frac{Eh}{8}\sqrt{2\pi} & 0 \\ 0 & 0 & 0 & 0 & \frac{Eh}{8}\sqrt{2\pi} \end{bmatrix} \begin{Bmatrix} \Delta\varphi_1 \\ \Delta\varphi_2 \\ \Delta w_3 \\ \Delta u_1 \\ \Delta u_2 \end{Bmatrix} \tag{9.8}$$

The values are interpolated to the crack tip (Fig. 6) using the following relationship

$$K = \frac{r_{AA'}}{r_{AA'} - r_{BB'}} \left(K^{BB'} - \frac{r_{BB'}}{r_{AA'}} K^{AA'} \right) \tag{9.9}$$

where $r_{AA'} = (5/6)l$; $r_{BB'} = (1/2)l$.

10. Numerical examples

To present the capability of the proposed method, several numerical examples are analysed. They include cracks in spherical and cylindrical shells.

10.1. Clamped and simply supported square spherical shells with a centre crack: uniformly loaded

Consider a square spherical shell with a centre crack shown in Fig. 7, with $b = 1$; $a/b = 0.2$, 0.4 and 0.6. Two cases of boundary conditions are considered in this example: clamped and simply supported on all sides. A uniform pressure is applied over the shell domain. Modulus of elasticity $E/p_0 = 210\,000$, Poisson's ratio $v = 0.3$ and ratio between the width and the shell thickness $b/h = 10$. The ratio between the width and the radius of curvature b/R is varied between 0.0 and 0.2, where $b/R = 0.0$ represent a flat plate.

For the analysis, eight elements per side of the shell, 12 elements for each crack surface are used, and 7×7 DRM domain points are used.

Figs. 8 and 9 show the displacements on the crack surface and along symmetry line for shell having $b/R = 0.01$. They are compared to half model using only displacement equations of BEM. As it can be seen, the results show good agreement between the two models.

At the top and bottom surfaces of the shell, that is $x_3 = \pm h/2$, stress intensity factors for this problem are as follows:

$$\left(1 \pm \frac{h}{2R}\right) K_{\mathrm{I}} = \frac{1}{h} K_{1m} \pm \frac{6}{h^2} K_{1b} \tag{10.1}$$

$$\left(1 \pm \frac{h}{2R}\right) K_{\mathrm{II}} = \frac{1}{h} K_{2m} \pm \frac{6}{h^2} K_{2b} \tag{10.2}$$

and

$$K_{\mathrm{III}} = 0 \tag{10.3}$$

On the other hand along the middle surface, that is $x_3 = 0$, the stress intensity factors are given by

$$K_{\mathrm{I}} = \frac{1}{h} K_{1m} \tag{10.4}$$

$$K_{\mathrm{II}} = \frac{1}{h} K_{2m} \tag{10.5}$$

and

$$K_{\mathrm{III}} = \frac{3}{2h} K_{3b} \tag{10.6}$$

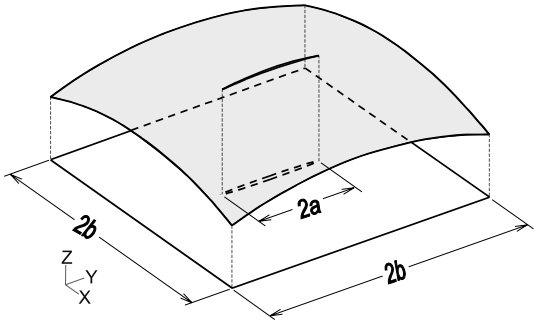

Fig. 7. Square spherical shell with a centre crack.

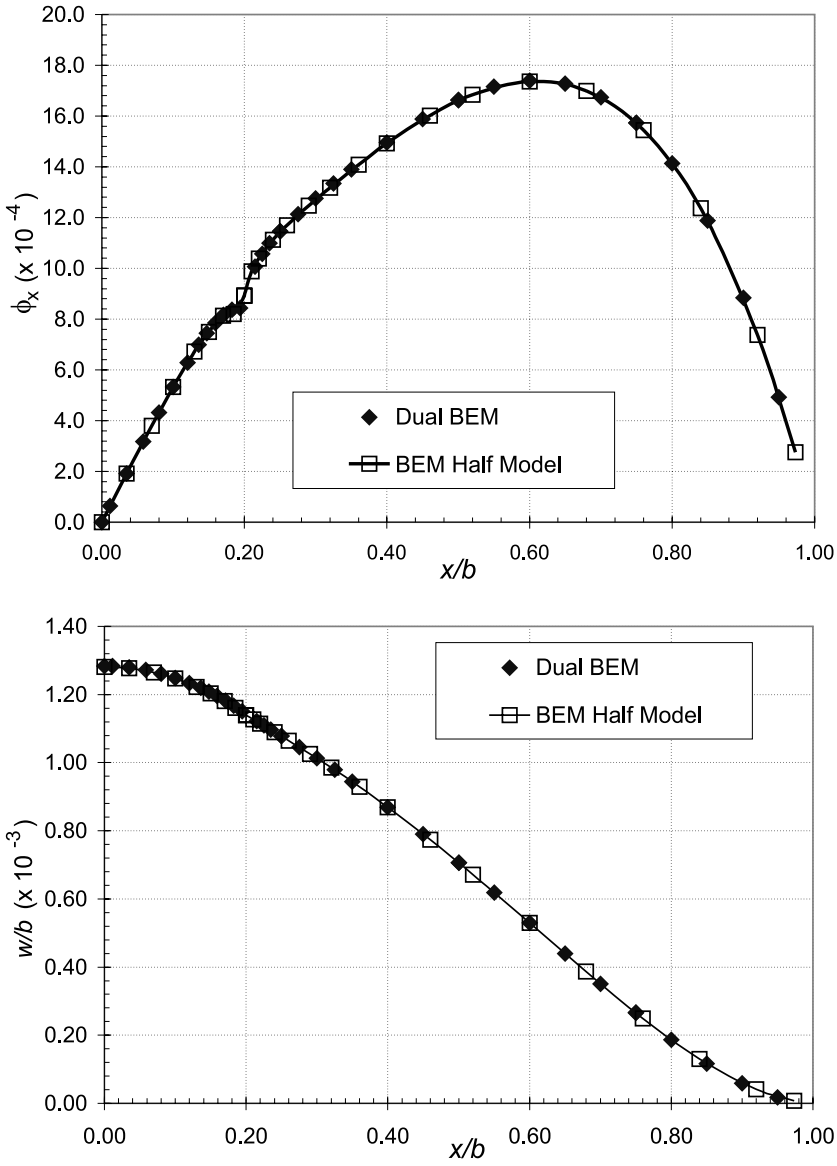

Fig. 8. Displacements on the crack surface and along the line of symmetry ($b/R = 0.01$, $a/b = 0.2$ and $b/h = 10$).

In this example, values of normalised K_{II} and K_{III} are very small (of order 10^{-7}), therefore this case can be considered as pure mode I. The normalised stress intensity factors for mode I, K_I due to bending and membrane obtained from the DBEM results are shown in Figs. 10 and 11. It can be seen from the results that as the radius of curvature R become smaller, the K_I due to membrane increases while the K_I due to bending decreases. This is because as the shell becomes deeper, more part of the pressure is transferred to membrane load. The results also show that as the $R \to \infty$, that is when the panel is flat, only K_I due to bending exist.

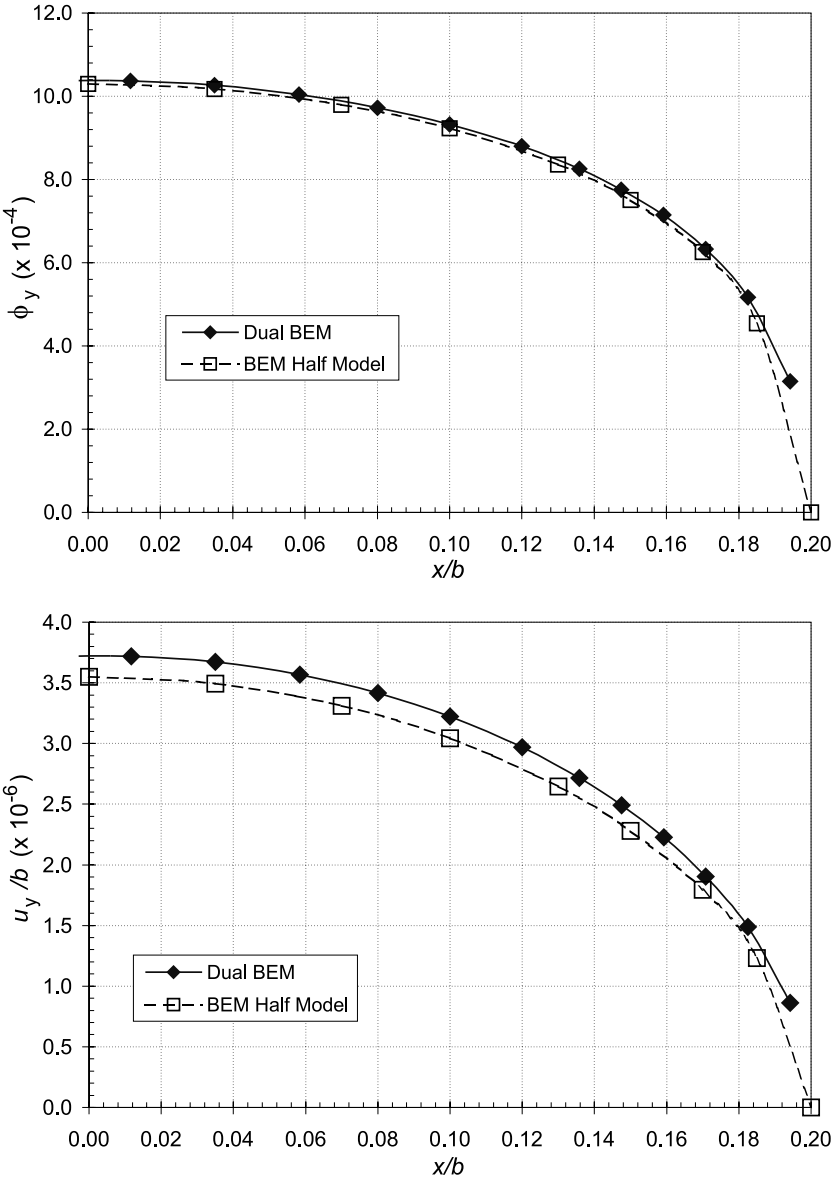

Fig. 9. Displacements on the crack surface and along the line of symmetry ($b/R = 0.01$, $a/b = 0.2$ and $b/h = 10$).

10.2. Clamped and simply supported square cylindrical shells with a centre crack: uniformly loaded

The second shell example considered here is a square cylindrical shell with a centre crack shown in Fig. 12 with $b = 1$; $a/b = 0.2$. A uniform pressure is applied over the shell domain. Modulus of elasticity of the material is chosen $E/p_0 = 210000$, Poisson's ratio $v = 0.3$ and shell thickness $b/h = 20$.

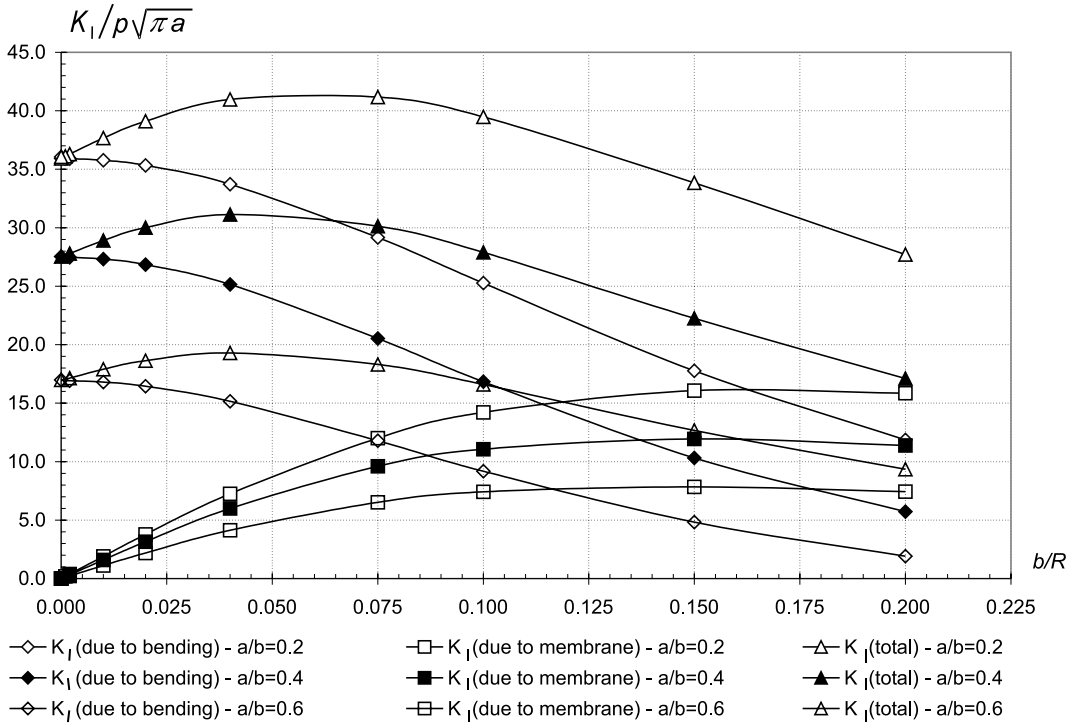

Fig. 10. Normalised K_I on the top surface of a clamped square spherical shell: uniform pressure.

For the DBEM analysis, eight elements per side of the shell and 12 elements for each crack surface are used, together with 7×7 DRM domain points. For comparison, half model of the shell is also analysed using 48 elements and 28 domain points (i.e. displacement BEM only), as well as FEM analysis using a quarter model of the shell with 3092 nodes and 1646 elements (Figs. 13 and 14).

Figs. 15 and 16 present the displacements on the crack surface and along the line of symmetry. Also presented are the BEM results obtained using the half model using only displacement equations and FEM results. As it can be seen, the results presented are in good agreements.

To study the effect of different type of shells and boundary conditions on the stress intensity factors, in this example clamped and simply supported square cylindrical shells are considered. A uniform load is applied over the shell domain. Modulus of elasticity of the material is chosen $E/p_0 = 210000$, Poisson's ratio $v = 0.3$ and the ratio between the width and shell thickness $b/h = 10$. Three different crack length, $a/b = 0.2$, 0.4 and 0.6 are analysed. Ratios between the width and the radius of curvature b/R_1 is varied between 0.0 and 0.2 and $b/R_2 = 0$.

As in the first example, the SIF values of normalised K_{II} and K_{III} obtained are very small (of order 10^{-7}), therefore this case can also be considered as pure mode I. The normalised stress intensity factors for mode I, K_I due to bending and membrane obtained from the DBEM results are shown in Figs. 17 and 18. Similar to the previous example, the results show that as the radius of curvature R_1 become smaller, the K_I due to membrane increases while the K_I due to bending decreases. The result also shows that as the $R_1 \to \infty$, that is when the panel is flat, only K_I due to bending exist.

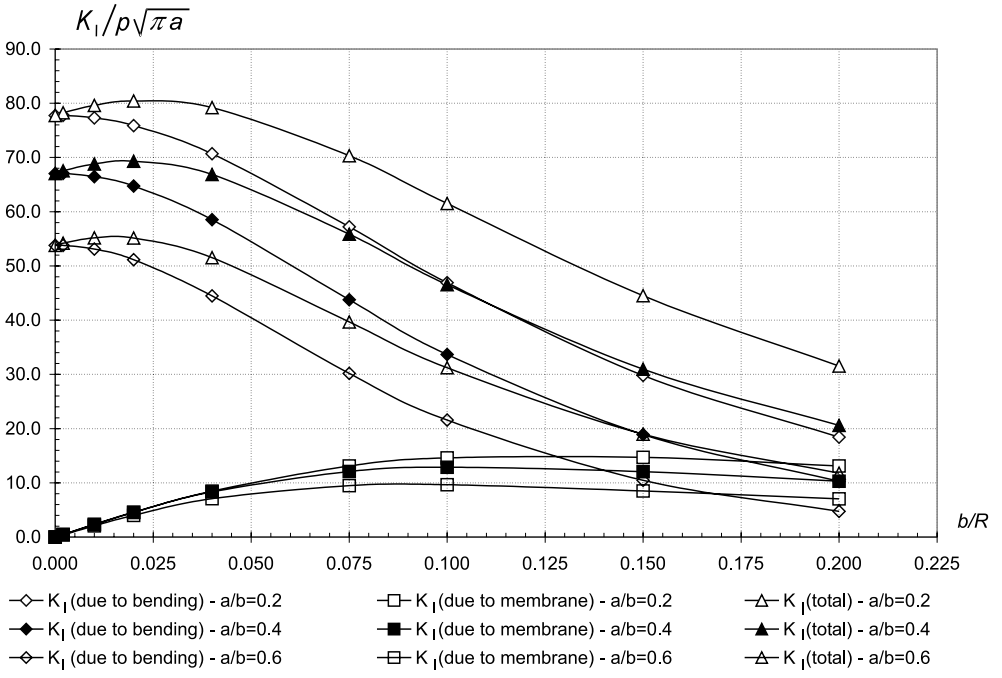

Fig. 11. Normalised K_I on the top surface of a simply supported square spherical shell: uniform pressure.

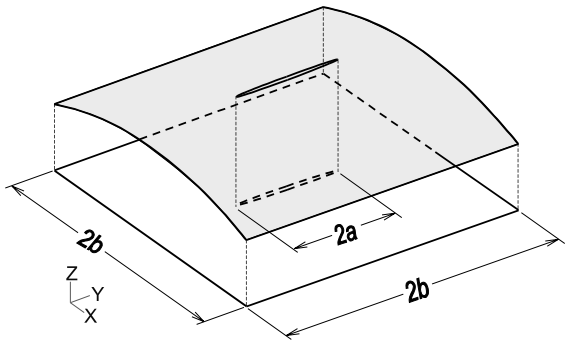

Fig. 12. Square cylindrical shell with a centre crack.

By comparing the results from spherical shell (example 10.1) and cylindrical shells (example 10.2), it can be seen that as the R_1 become smaller, the total stress intensity factor decreases faster in spherical shell. It can also be seen in the results that as the $R_1 \to \infty$, in both examples the stress intensity factors are approaching those of a flat plate due to bending (see Dirgantara, 2000).

With the capability of computer today, it takes only a few minute computer time for solving computational model of structures (in this case, using Pentium III 650 MHz with 256 MB RAM, this example was solved in less than two minutes). Therefore the main issue of computer modelling of structure is the time spent on data preparation.

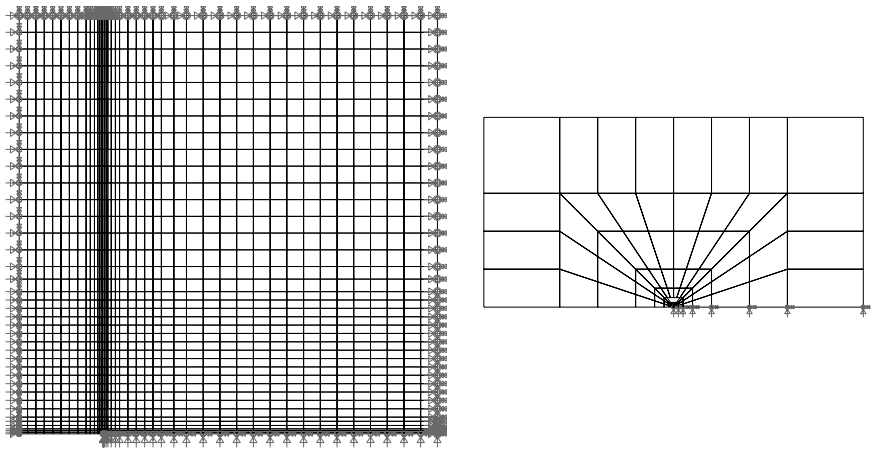

Fig. 13. FEM – quarter model of centre crack in cylindrical shell: 3092 nodes, 1646 elements.

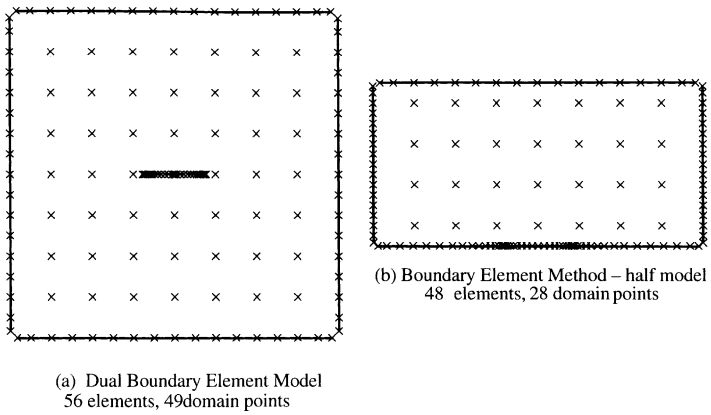

Fig. 14. Boundary element models for a centre crack in cylindrical shell: (a) DBEM; (b) BEM – half model.

10.3. Symmetric cracks emanating from a hole in a square cylindrical shells

As the last example, consider a symmetric cracks emanating from a hole in a square cylindrical shell $b = 1$; $a/b = 0.2$ and 0.5 as shown in Fig. 19. The shell is simply supported on two sides. A uniform load is applied over the shell domain. Modulus of elasticity $E/p_0 = 210000$ and Poisson's ratio $v = 0.3$. Ratio between hole size and shell width is $r/b = 0.1$, and the shell width to thickness ratio is $b/h = 10$. The value of $b/R_2 = 0.0$ and b/R_1 is varied between 0.0 and 0.2, where $b/R_1 = 0.0$ represent a flat plate.

For the analysis, a total of 132 elements, that is eight boundary elements per side of the shell, 20 elements for the hole and 20 elements for each crack surface, and 7×7 DRM domain points are used.

The normalised stress intensity factors for mode I, K_I due to bending and membrane are shown in Fig. 20. The normalisation factors used here are the same as the ones used in the cylindrical shell example. Similar to the previous example, the results show that as the radius of curvature R_1 become smaller, the K_I due to membrane increases while the K_I due to bending decreases. The results also show that as the

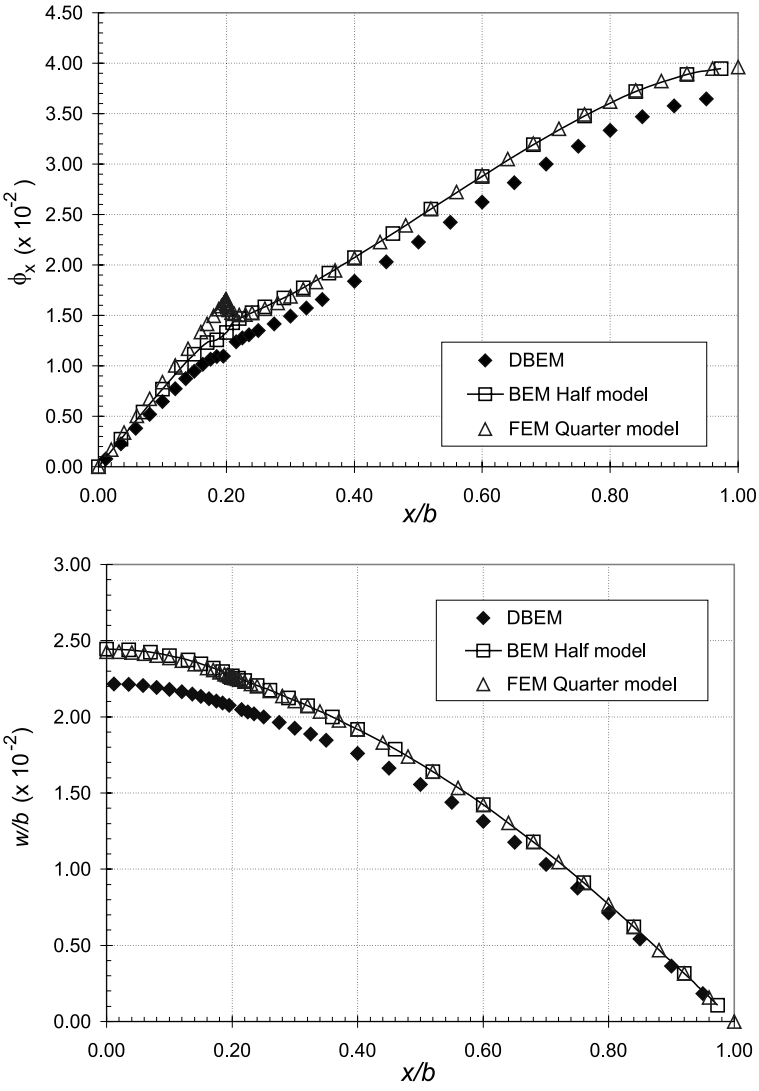

Fig. 15. Displacements on the crack surface and along the line of symmetry ($b/R_2 = 0.01$, $a/b = 0.2$ and $b/h = 20$).

$R_1 \to \infty$, that is when the panel is flat, only K_I due to bending exist, and the value is the same as the one which is obtained for plate bending example (see Dirgantara, 2000).

11. Conclusion

In this paper, the dual boundary integral equations were derived for the shear deformable shell theory. Domain integrals were transformed to boundary integral with the aid of the DRM, using radial basis function $1 + r$ and its derivatives. To model accurately displacement field near the crack tip, special crack tip elements were developed. These elements were used for the evaluation of SIFs using a CSDE technique.

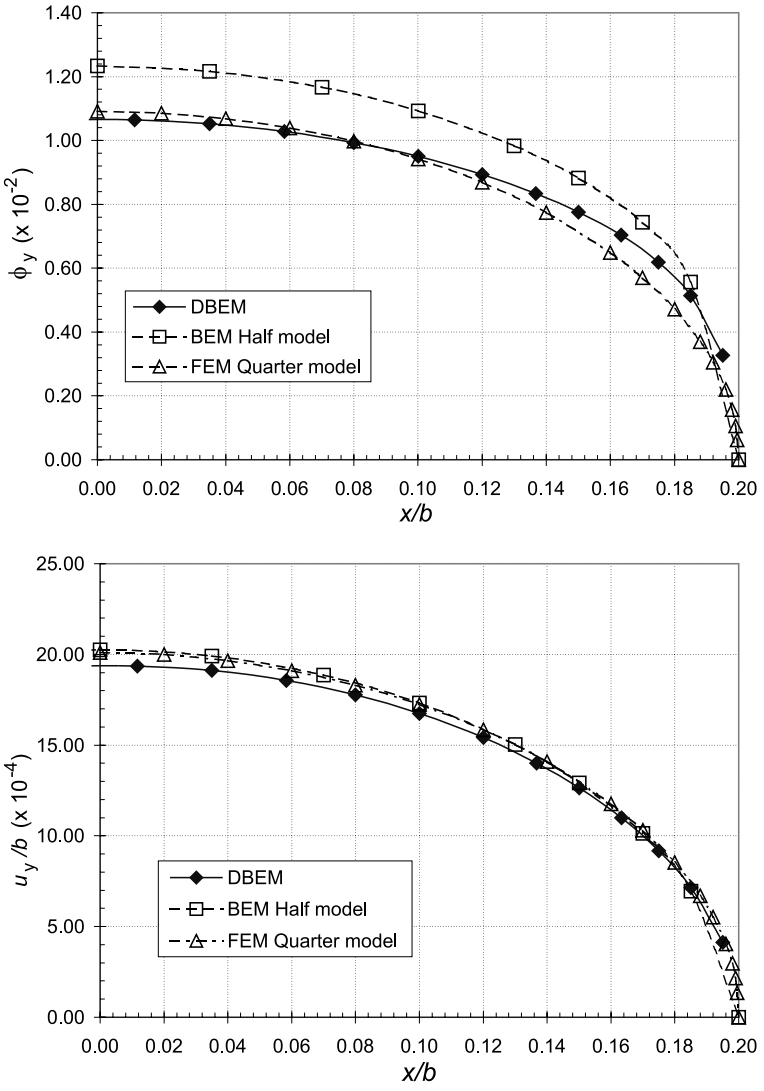

Fig. 16. Displacements on the crack surface and along the line of symmetry ($b/R_2 = 0.01$, $a/b = 0.2$ and $b/h = 20$).

Several examples were solved, and the results demonstrated the accuracy and the validity of the present formulations.

Appendix A

A.1. Particular solutions for two-dimensional plane stress

An expression for displacement particular solution $\hat{u}^{\gamma}_{m\alpha}$ can be obtained in polar coordinates with the use of the Galerkin vector $G_{\alpha\beta}$ as

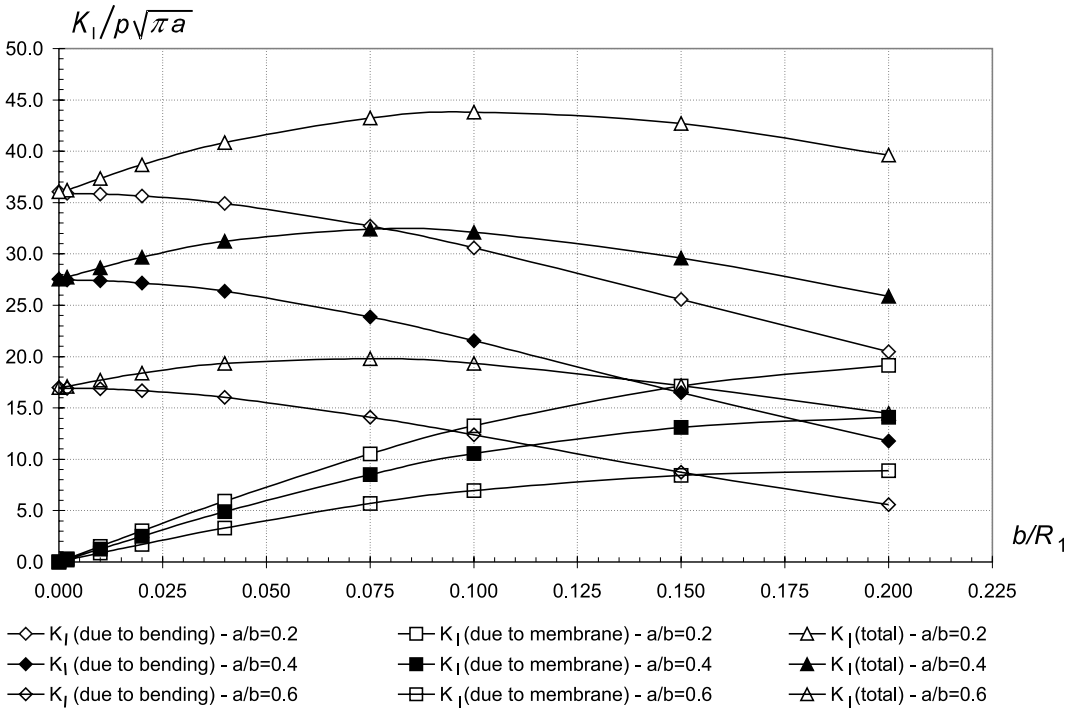

Fig. 17. Normalised K_1 on the top surface of a clamped square cylindrical shell: uniform pressure.

$$\hat{u}^{\gamma}_{m\alpha}(r) = G^{\gamma}_{\beta\alpha,\gamma\gamma}(r) - \frac{1+v}{2} G^{\gamma}_{\gamma\alpha,\beta\gamma}(r) \tag{A.1}$$

where $G_{\alpha\beta}$ satisfies

$$\nabla^4 G^{\gamma}_{\beta\alpha} + \frac{2}{(1-v)B}\frac{x_\gamma}{r}\delta_{\gamma\beta} = 0 \tag{A.2}$$

and a solution is determined by

$$G^{\gamma}_{\beta\alpha} = -\frac{r^3 x_\gamma}{45(1-v)B}\delta_{\alpha\beta} \tag{A.3}$$

Substituting Eq. (A.3) into Eq. (A.1), then the particular solution for displacements can be arranged as

$$\begin{aligned} \hat{u}^1_{m1} &= -\frac{2}{(1-v)B}\left[\frac{r x_1}{3} - \frac{1+v}{30}\left(\frac{x_1^3}{r} + 3x_1 r\right)\right] \\ \hat{u}^1_{m2} &= \frac{(1+v)}{15(1-v)B}\left(\frac{x_1^2 x_2}{r} + x_2 r\right) \end{aligned} \tag{A.4}$$

and using strain-displacement relationships for 2-D plane stress, the strains are obtained as

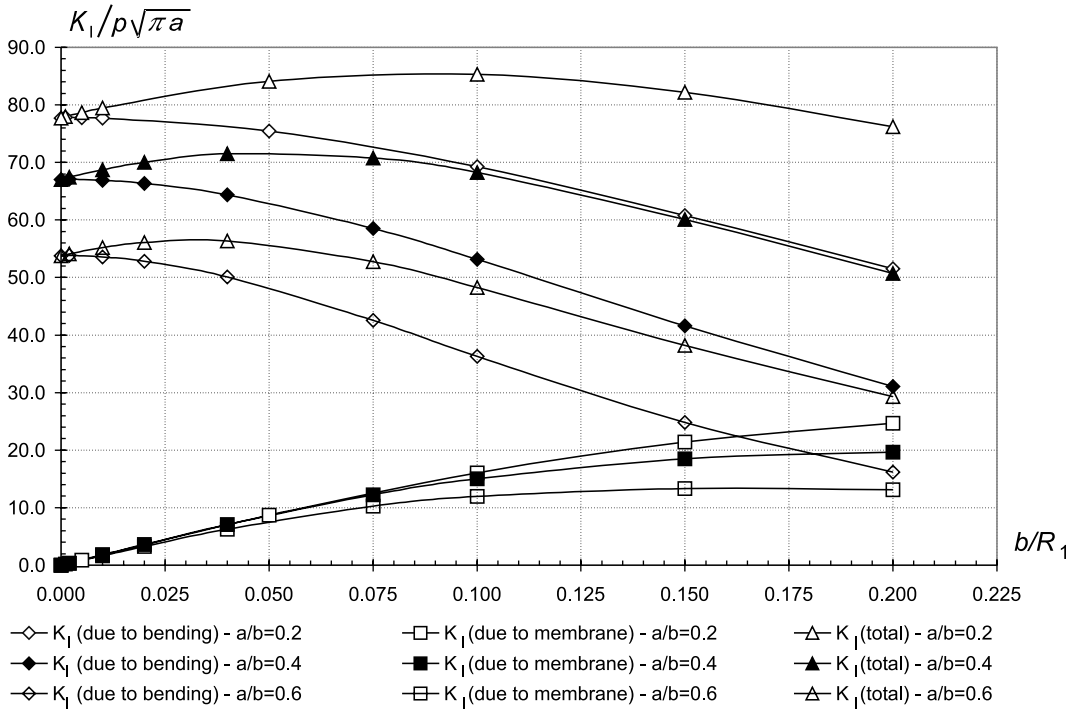

Fig. 18. Normalised K_1 on the top surface of a simply supported square cylindrical shell: uniform pressure.

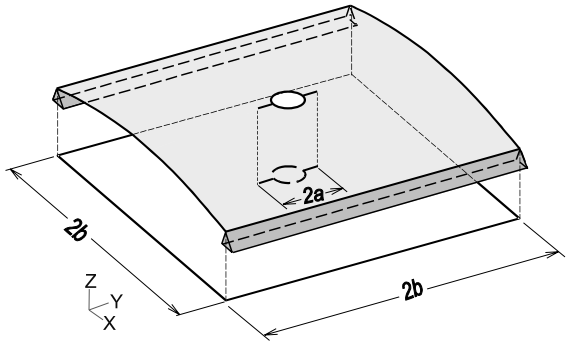

Fig. 19. Symmetric cracks emanating from a hole in a square cylindrical shell, simply supported on two sides, subjected to uniform pressure.

$$\hat{\varepsilon}^1_{m11} = -\frac{2}{(1-v)}\left[\left(\frac{x_1^2}{r}+\frac{r}{3}\right)-\frac{1+v}{30}\left(-\frac{x_1^4}{r^3}+\frac{6x_1^2}{r}+3r\right)\right]$$
$$\hat{\varepsilon}^1_{m12} = -\frac{2}{(1-v)}\left[\frac{x_1x_2}{6r}-\frac{1+v}{30}\left(-\frac{x_1^3x_2}{r^3}+\frac{3x_1x_2}{r}\right)\right] \tag{A.5}$$
$$\hat{\varepsilon}^1_{m22} = \frac{2}{(1-v)}\frac{1+v}{30}\left(-\frac{x_1^2x_2^2}{r^3}+2r\right)$$

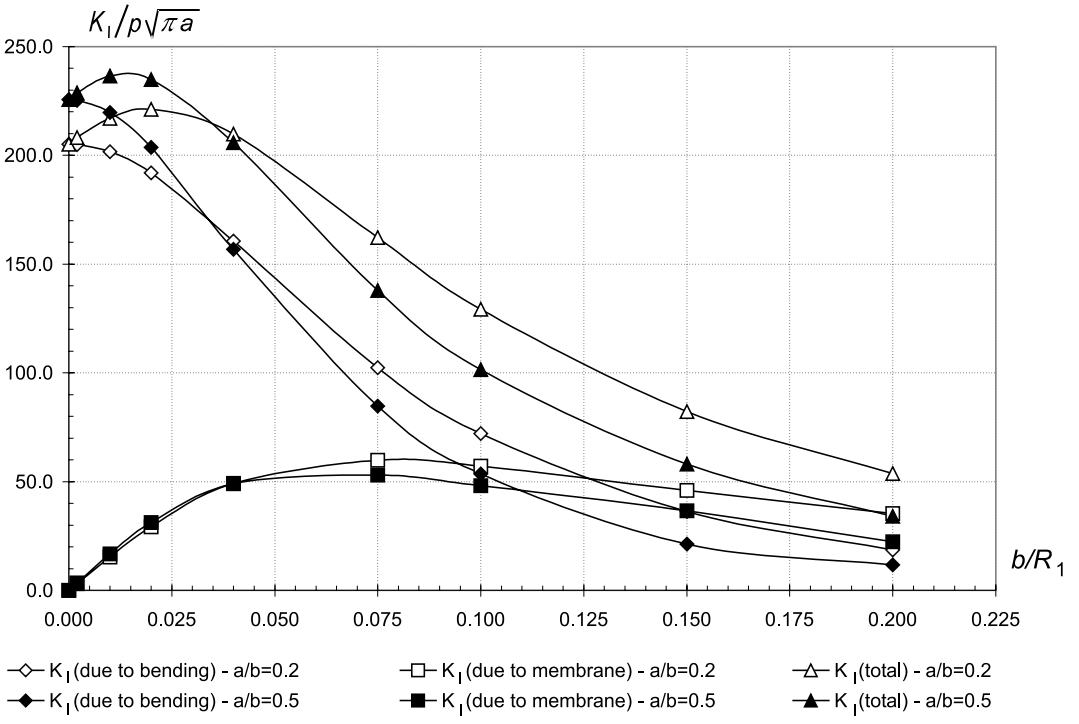

Fig. 20. Normalised K_I on the top surface of symmetric cracks emanating from a hole in a square cylindrical shell, simply supported on two sides, subjected to uniform pressure.

The particular solution for membrane stress resultant can be derived by substituting Eq. (A.5) into the stress resultant-strain relationships for 2-D plane stress to give:

$$\begin{aligned}\hat{N}^1_{m11} &= B\left[(1-v)\hat{\varepsilon}^1_{m11} + v\hat{\varepsilon}^1_{m\alpha\alpha}\right]\\ \hat{N}^1_{m12} &= B(1-v)\hat{\varepsilon}^1_{m12}\\ \hat{N}^1_{m22} &= B\left[(1-v)\hat{\varepsilon}^1_{m22} + v\hat{\varepsilon}^1_{m\alpha\alpha}\right]\end{aligned} \tag{A.6}$$

and the particular solutions of traction are obtained from

$$\hat{t}^1_{m\alpha} = \hat{N}^1_{m\alpha\beta} n_\beta \tag{A.7}$$

In the same way, displacement particular solutions $\hat{u}^2_{m\alpha}$ can be obtained as follows:

$$\begin{aligned}\hat{u}^2_{m1} &= \frac{(1+v)}{15(1-v)B}\left(\frac{x_2^2 x_1}{r} + x_1 r\right)\\ \hat{u}^2_{m2} &= -\frac{2}{(1-v)B}\left[\frac{r x_2}{3} - \frac{1+v}{30}\left(\frac{x_2^3}{r} + 3x_2 r\right)\right]\end{aligned} \tag{A.8}$$

and the strains are

$$\begin{aligned}
\hat{\varepsilon}^2_{m11} &= \frac{2}{(1-v)}\frac{1+v}{30}\left(-\frac{x_1^2x_2^2}{r^3}+2r\right)\\
\hat{\varepsilon}^2_{m12} &= -\frac{2}{(1-v)}\left[\frac{x_1x_2}{6r}-\frac{1+v}{30}\left(-\frac{x_2^3x_1}{r^3}+\frac{3x_1x_2}{r}\right)\right]\\
\hat{\varepsilon}^2_{m22} &= -\frac{2}{(1-v)}\left[\left(\frac{x_2^2}{r}+\frac{r}{3}\right)-\frac{1+v}{30}\left(-\frac{x_2^4}{r^3}+\frac{6x_2^2}{r}+3r\right)\right]
\end{aligned} \tag{A.9}$$

The particular solution for membrane stress resultant are

$$\begin{aligned}
\hat{N}^2_{m11} &= B\left[(1-v)\hat{\varepsilon}^2_{m11}+v\hat{\varepsilon}^2_{m\alpha\alpha}\right]\\
\hat{N}^2_{m12} &= B(1-v)\hat{\varepsilon}^2_{m12}\\
\hat{N}^2_{m22} &= B\left[(1-v)\hat{\varepsilon}^2_{m22}+v\hat{\varepsilon}^2_{m\alpha\alpha}\right]
\end{aligned} \tag{A.10}$$

and finally the particular solutions of traction are obtained from

$$\hat{t}^2_{m\alpha} = \hat{N}^2_{m\alpha\beta}n_\beta \tag{A.11}$$

A.2. Particular solutions for plate bending

Governing equation for shear deformable plate bending problem can be written as

$$\hat{\mathbf{w}} = \mathbf{H}\mathbf{e}\varphi \tag{A.12}$$

where particular solutions of displacement $\hat{\mathbf{w}} = \{\hat{w}_1, \hat{w}_2, \hat{w}_3\}^\top$, $\mathbf{e} = \{e_1, e_2, e_3\}^\top$ is arbitrary constant vector and components of matrix $\mathbf{H}$ are

$$\begin{aligned}
H_{\alpha\beta} &= 2\delta_{\alpha\beta}\nabla^4 - [(1+v)\nabla^2+(1-v)\lambda^2)]\frac{\partial^2}{\partial x_\alpha \partial x_\beta}\\
H_{3\alpha} &= -H_{\alpha 3} = -(1-v)(\nabla^2-\lambda^2)\frac{\partial}{\partial x_\alpha}\\
H_{33} &= (\nabla^2-\lambda^2)[2\nabla^2-(1-v)\lambda^2]/\lambda^2
\end{aligned} \tag{A.13}$$

The function φ can be defined from Eq. (A.12) such that

$$D(1-v)(\nabla^2-\lambda^2)\nabla^4\varphi + F(r) = 0 \tag{A.14}$$

If $e_1 = 0$, $e_2 = 0$ and $e_3 = 1$, the particular solution used in Eq. (6.4) can be written as

$$\begin{aligned}
\hat{w}_{m\alpha} &= -\frac{1}{D}\frac{\partial\varphi}{\partial x_\alpha}\\
\hat{w}_{m3} &= \frac{1}{(1-v)D\lambda^2}[2\nabla^2\varphi-(1-v)\lambda^2\psi]
\end{aligned} \tag{A.15}$$

where

$$\nabla^4\varphi(r) + F(r) = 0 \tag{A.16}$$

The particular solutions of moment and shear force can be determined from shear deformable plate bending stress resultant-displacement relationship. The tractions on the boundary can be obtained by

$$\hat{p}_{m\alpha} = \hat{M}_{\alpha\beta}n_\beta, \quad \hat{p}_{m3} = \hat{Q}_\alpha n_\alpha \tag{A.17}$$

If radial basis function $F(r) = 1 + r$, The function $\varphi(r)$ can be solved from Eq. (A.16)

$$\varphi(r) = -\left(\frac{r^4}{64} + \frac{r^5}{225}\right) \tag{A.18}$$

and the rotations and deflection can be deduced

$$\begin{aligned}
\hat{w}^3_{m1} &= -\left(\frac{1}{16} + \frac{r}{45}\right)\frac{x_1 r^2}{D} \\
\hat{w}^3_{m2} &= -\left(\frac{1}{16} + \frac{r}{45}\right)\frac{x_2 r^2}{D} \\
\hat{w}^3_{m3} &= -\left(\frac{1}{2} + \frac{2r}{9}\right)\frac{r^2}{(1-\nu)\lambda^2 D} + \left(\frac{1}{64} + \frac{r}{225}\right)\frac{1}{D}
\end{aligned} \tag{A.19}$$

The particular solutions of moments $\hat{M}_{\alpha\beta}$ and shear forces $\hat{Q}_\beta$ can be determined by from shear deformable plate bending stress resultant-displacement relationship to give

$$\begin{aligned}
\hat{M}^3_{m11} &= -\left[\left(\frac{1}{8} + \frac{r}{15}\right)\left(x_1^2 + \nu x_2^2\right) + (1+\nu)\left(\frac{r^2}{16} + \frac{r^3}{45}\right)\right] \\
\hat{M}^3_{m12} &= -(1+\nu)\left(\frac{1}{8} + \frac{r}{15}\right)(x_1 x_2) \\
\hat{M}^3_{m22} &= -\left[\left(\frac{1}{8} + \frac{r}{15}\right)\left(\nu x_1^2 + x_2^2\right) + (1+\nu)\left(\frac{r^2}{16} + \frac{r^3}{45}\right)\right] \\
\hat{Q}^3_{m1} &= -\frac{x_1}{2}\left(1 + \frac{2r}{3}\right) \\
\hat{Q}^3_{m2} &= -\frac{x_2}{2}\left(1 + \frac{2r}{3}\right)
\end{aligned} \tag{A.20}$$

and the tractions on the boundary can be obtained from relationships in Eq. (A.17).

For the derivative of function $F_{,\alpha} = x_\alpha / r$, the solution $\varphi^\alpha(r)$ can be found

$$\varphi^\alpha(r) = -\frac{r^3 x_\alpha}{45} \tag{A.21}$$

and particular solutions $\hat{w}^\alpha_{mk}$ are

$$\begin{aligned}
\hat{w}^1_{m1} &= -(3x_1^2 + r^2)\frac{r}{45D} \\
\hat{w}^1_{m2} &= -\frac{x_1 x_2 r}{15D} \\
\hat{w}^1_{m3} &= -[30 - (1-\nu)\lambda^2 r^2]\frac{r x_1}{45(1-\nu)\lambda^2 D}
\end{aligned} \tag{A.22}$$

and the particular solutions of moments $\hat{M}_{\alpha\beta}$ and shear forces $\hat{Q}_\beta$ are

$$\begin{aligned}
\hat{M}^1_{m11} &= -\frac{x_1}{15}\left[\nu\left(\frac{x_1^2}{r}+3r\right)+\left(\frac{x_2^2}{r}+r\right)\right]\\
\hat{M}^1_{m12} &= -(1-\nu)\frac{x_2}{15}\left(\frac{x_1^2}{r}+r\right)\\
\hat{M}^1_{m22} &= -\frac{x_1}{15}\left[\nu\left(\frac{x_1^2}{r}+3r\right)+\left(\frac{x_2^2}{r}+r\right)\right]\\
\hat{Q}^1_{m1} &= -\frac{1}{3}\left(\frac{x_1^2}{r}+r\right)\\
\hat{Q}^1_{m2} &= -\frac{1}{3}\frac{x_1x_2}{r}
\end{aligned} \tag{A.23}$$

for $\alpha = 1$, and

$$\begin{aligned}
\hat{w}^2_{m1} &= -\frac{x_1x_2r}{15D}\\
\hat{w}^2_{m1} &= -(3x_2^2+r^2)\frac{r}{45D}\\
\hat{w}^2_{m3} &= -[30-(1-\nu)\lambda^2r^2]\frac{rx_2}{45(1-\nu)\lambda^2D}
\end{aligned} \tag{A.24}$$

and the particular solutions of moments $\hat{M}_{\alpha\beta}$ and shear forces $\hat{Q}_\beta$ are

$$\begin{aligned}
\hat{M}^2_{m11} &= -\frac{x_2}{15}\left[\nu\left(\frac{x_1^2}{r}+r\right)+\left(\frac{x_2^2}{r}+3r\right)\right]\\
\hat{M}^2_{m12} &= -(1-\nu)\frac{x_1}{15}\left(\frac{x_2^2}{r}+r\right)\\
\hat{M}^2_{m22} &= -\frac{x_2}{15}\left[\nu\left(\frac{x_1^2}{r}+r\right)+\left(\frac{x_2^2}{r}+3r\right)\right]\\
\hat{Q}^2_{m1} &= -\frac{1}{3}\frac{x_1x_2}{r}\\
\hat{Q}^2_{m2} &= -\frac{1}{3}\left(\frac{x_2^2}{r}+r\right)
\end{aligned} \tag{A.25}$$

for $\alpha = 2$.

References

Ahmadi-Brooghani, S.Y., Wearing, J.L., 1996. The application of the dual boundary element method in linear elastic crack problem in plate bending. Boundary Element Methods XVIII, In: Brebbia, C.A., Martins, J.B., Aliabadi, M.H., Haie, N., (Eds.), Computational Mechanics Publications, Southampton, pp. 429–438.

Aliabadi, M.H., 1997a. Boundary element formulations in fracture mechanics. Appl. Mech. Rev. 50 (2), 83–96.

Aliabadi, M.H., 1997b. A new generation of boundary element formulations in fracture mechanics. Int. J. Fract. 86, 91–125.

Aliabadi, M.H., Hall, W.S., Phemister, T.G., 1985. Taylor expansion for singular kernels in the boundary element method. Int. J. Numer. Meth. Engng. 21, 2221–2236.

Aliabadi, M.H., Rooke, D.P., 1991. Numerical fracture mechanics. Kluwer Academic Publisher, Dordrecht, The Netherlands.

Barsoum, R.S., Loomis, R.W., Stewart, B.D., 1979. Analysis of through crack in cylindrical shells by quarter point elements. Int. J. Fract. 15 (3), 259–280.

Beskos, D.E., 1991. Static and dynamic analysis of shells. In: Beskos, D.E. (Ed.), Boundary Element Analysis of Plate and Shells. Spinger-Verlag, Berlin, pp. 93–140.

Budiman, H.T., Lagace, P.A., 1997. Non dimensional parameters for geometric nonlinear effects in pressurized cylinders with axial cracks. J. Appl. Mech. 64, 401–406.

Dirgantara, T., 2000. Boundary element analysis of crack in shear deformable plates and shells. Ph.D. Thesis. Department of Engineering, Queen Mary and Wesfield College, University of London.

Dirgantara, T., Aliabadi, M.H., 1999. A new boundary element formulation for shear deformable shells analysis. Int. J. Numer. Meth. Engng. 5, 1257–1275.

Dirgantara, T., Aliabadi, M.H., 2000. Crack growth analysis of plates loaded by bending and tension using dual boundary element method. Int. J. Fract. 105 (1), 27–47.

Delale, F., Erdogan, F., 1979a. Transverse shear effect in a circumferencially cracked cylindrical shell. Quart. Appl. Mech. 37, 239–258.

Delale, F., Erdogan, F., 1979b. Effect of transverse shear and material orthotopy in a cracked spherical cap. Int. J. Solids Struct. 15, 907–926.

Ehlers, R., 1986. Stress intensity factors and crack opening areas for axial through cracks in hollow cylinders under internal pressure loading. Engng. Fract. Mech. 25 (1), 63–77.

Erdogan, F., Kibler, J.J., 1968. Cylindrical and spherical shells with crack. Int. J. Fract. Mech. 5 (3), 229–237.

Folias, E., 1965a. A finite line crack in a pressurized spherical shell. Int. J. Fract. Mech. 1, 20–46.

Folias, E., 1965b. An axial crack in a pressurized cylindrical shell. Int. J. Fract. Mech. 1, 20–46.

Karam, V.J., Telles, J.C.F., 1988. On boundary elements for Reissner's plate theory. Engng. Anal. 5, 21–27.

Krenk, S., 1978. Influence of transverse shear on an axial crack in a cylindrical shell. Int. J. Fract. 14 (2), 123–143.

Lu, P., Huang, M., 1991. Computation of the fundamental solution for shallow shells involving shear deformation. Int. J. Solids Struct. 28 (5), 631–645.

Lu, P., Huang, M., 1992. Boundary element analysis of shallow shells involving shear deformation. Int. J. Solids Struct. 29 (10), 1273–1282.

Mi, Y., Aliabadi, M.H., 1994. Discontinuous crack-tip elements: application to 3-D boundary element method. Int. J. Fract. 67, R67–R71.

Murakami, Y., et al. (Eds.), 1987. Stress Intensity Factors Handbook. Pergamon Press, New York.

Naghdi, P.M., 1956. On the theory of thin elastic shells. Quart. Appl. Math. 14, 369–380.

Portela, A., Aliabadi, M.H., 1992. The dual boundary element method : effective implementation for crack problems. Int. J. Numer. Meth. Engng. 33, 1269–1287.

Rashed, Y.F., Aliabadi, M.H., Brebbia, C.A., 1998. Hypersingular boundary element formulation for Reissner plates. Int. J. Solids Struct. 35 (18), 2229–2249.

Reissner, E., 1947. On bending of elastic plates. Quart. Appl. Math. 5, 55–68.

Salgado, N.K., Aliabadi, M.H., 1998. Boundary element analysis of cracked stiffened sheets reinforced by adhesively bonded patches. Int. J. Numer. Meth. Engng. 42 (2), 195–217.

Sih, G.C., Hagendorf, H.C., 1977. On cracks in shells with shear deformation. In: Sih, G.C. (Ed.), Mechanics of Fracture Plate and Shells with Cracks, vol. 3. Noordhoff International Publishing, Leyden, pp. 201–229.

Telles, J.C.F., 1987. A self-adaptive coordinate transformation for efficient numerical evaluation of general boundary element integrals. Int. J. Numer. Meth. Engng. 24, 959–973.

Van der Weeën, F., 1982. Application of the boundary integral equation method to Reissner's plate model. Int. J. Numer. Meth. Engng. 18, 1–10.

Wen, P.H., Aliabadi, M.H., Young, A., 2000. Plane stress and plate bending coupling in BEM analysis of shallow shells. Int. J. Numer. Meth. Engng. 48, 1107–1125.